HSE
Health & Safety Executive

The static strength of cracked joints in tubular members

Prepared by **UMIST**
for the Health and Safety Executive

OFFSHORE TECHNOLOGY REPORT
2001/080

HSE
Health & Safety Executive

The static strength of cracked joints in tubular members

Professor F M Burdekin FREng FRS
UMIST
The Manchester Centre for Civil and Construction Engineering
Sackville Street
Manchester
M60 1QD
United Kingdom

HSE BOOKS

First published 2002

ISBN 0 7176 2301 7

SUMMARY

This report reviews the research which has been carried out from the 1980s to 2000 into the effect of cracks on the static strength of tubular joints. The effects of cracks on both plastic collapse and fracture are considered for a range of different types of joint geometry. The main geometries considered are T,Y,DT and K tubular joints with cracks around the weld toe in the chord and plain brace members with circumferential cracks. The information available consists of experimental test data and the results of a series of finite element analysis investigations. The fracture considerations are divided into brittle fracture and ductile tearing fracture and procedures are outlined for estimating the strength of tubular joints for these different circumstances. Analyses have been carried out on some recent data which confirm that the procedures recommended give safe estimates of the strength of cracked joints.

CONTENTS LIST

1. INTRODUCTION

Tubular members and joints in offshore structures are normally designed to resist the maximum storm wave for the location as static strength and to resist the spectrum of wave loading for fatigue strength. The basis of the static design is one of the design codes, such as API RP2A[(1)], supplemented by requirements such as the HSE Guidance Notes[(2)]. The latter are based primarily on the analysis of experimental tests on model scale joints, for which a substantial database has now been established.

The design equations for the former HSE Guidance Notes gave the following form for the characteristic strength of simple tubular joints:

$$P_k = Q_u Q_f \frac{F_y T^2 K_a}{\sin\theta}$$

$$M_{ki}, M_{ko} = Q_u Q_f \frac{F_y T^2 d}{\sin\theta}$$

where Q_u is a strength factor which varies with type of joint and loading as given in the following table and Q_f is a factor to allow for the presence of axial and moment loads in the chord:

Load Direction	**Coefficient Q_u for various Joint Design Classifications**		
	Y	**K**	**X**
Axial Compression	$(2+20\beta)\sqrt{Q_\beta}$	$(2+20\beta).Q_g.\sqrt{Q_\beta}$	$(2.5+14\beta)Q_\beta$
Axial Tension	$(8+22\beta)$	$(8+22\beta).Q_g$	$(7+17\beta).Q_\beta$
In-plane bending	$5\beta\gamma^{1/2}\sin\theta$		
Out-of-plane bending	$(1.6+7\beta)Q_\beta$		$(2.5+14\beta)\sqrt{Q_\beta}$

where

$$Q_\beta = 1.0 \quad \text{for } \beta \le 0.6$$

$$Q_\beta = \frac{0.3}{\beta(1-0,.833\beta)} \quad \text{for } \beta \ge 0.6$$

$$\text{and} \quad K_a = (1+1/\sin\theta)/2$$

and $Q_g = 1.7 - 0.9\,\tau^{0.9}$ but should not be taken as less than 1.0.

Updated versions of these equations for DT joints have been recommended as follows[(3)]:

DT joints in tension – $P = F_y T^2.Q_u$ – with values of Q_u given in the following table:

Failure Criterion	**Mean**	**Characteristic**
First crack	33.3β for $\beta \le 0.9$ $30.4 + (\beta - 0.9)(24.6\gamma - 318)$ for $\beta > 0.9$	23β for $\beta \le 0.9$ $21 + (\beta - 0.9)(17\gamma - 220)$ for $\beta > 0.9$
Ultimate	$46.7\beta - 2.5$ for $\beta \le 0.9$ $39.8 + (\beta - 0.9)(36.4\gamma - 324)$ for $\beta > 0.9$	$41\beta - 2.2$ for $\beta \le 0.9$ $35 + (\beta - 0.9)(32\gamma - 285)$ for $\beta > 0.9$

DT joints under OPB – $M = F_y T^2 .d.Q_u$ – with values of Q_u given in the following table:

Mean	Characteristic
$3.64\gamma^{(0.5\beta^2)}$	$3.2\gamma^{(0.5\beta^2)}$

DT joints under IPB – $M = F_y T^2 .d.Q_u$ – with values of Q_u given in the following table:

Mean	Characteristic
$5.5\ \beta\gamma^{0.5}$	$4.5\ \beta\gamma^{0.5}$

The above formulae apply to sound joints without defects. It should be noted that the HSE equations are based on maximum load from an extensive database of experimental test results on of the different geometries and loadings concerned, generally at a scale smaller than the full scale of actual structures. Alternative formulae are available, for example those from API[(1)], which are based on the first observance of cracking in the same series of tests as used for the HSE equations. The API equations thus lead to somewhat lower design loads than the HSE equations. It is also important to recognise that the mode of failure may be different in different types of joint and under different types of loading. In particular joints under tension usually fail by tearing and fracture failure, whilst failure of joints under compression loading may occur by buckling of the walls of the tubular members. Thus sound T and Y joints are usually weaker in compression than in tension. In K joints, where one brace is in tension and one brace in compression, the ultimate strength of sound joints is usually intermediate between that of corresponding Y joints in tension or compression because the tension member provides some support against buckling through the ligament of material in the gap region between the braces.

In practice, defects may occur in such joints either at the time of fabrication or in service. Although critical welded joints are subject to thorough non-destructive testing immediately after fabrication, there remains the requirement for acceptance levels to be determined and the possibility of defects escaping detection. Offshore structures are subjected to repeated wave loading and hence there is the possibility of fatigue cracks developing in service.

It is therefore important to be able to assess the effect of defects on the strength of tubular joints. A number of research programmes have now been carried out into the behaviour of cracked tubular joints as summarised in the next section.

2. RESEARCH INTO STRENGTH OF CRACKED TUBULAR JOINTS

Following major research programmes into the fatigue performance of tubular joints in the 1970s some limited investigations were carried out into the strength of cracked joints by testing the remaining strength of the fatigue specimens, notably by Kurobane[4] and by Gibstein[5,6]. The tests by Gibstein were mainly T joints under axial tension and are notable for using a combination of materials and test temperature to produce failure by brittle fracture. Tests designed to produce failure by brittle fracture were also carried out by Machida et al.[7] These investigations were on materials typical of Grade 355 steel properties.

A series of ongoing research programmes into assessment of defects in tubular joints was started at UMIST in 1985 initially as a joint universities' programme with Glasgow University and University College London, but later with TWI and in separate independent projects supported by HSE and industrial partners.[8-13]. These programmes were the first serious effort to combine finite element analysis, fracture mechanics procedures and model scale testing to provide guidance on the assessment of the effect of cracks on the ultimate strength of tubular joints.

The UMIST work by Frodin[8] involved a combination of finite element analysis and model scale experimental tests on double T joints with β values of 0.34, 0.54 and 0.82 with through thickness cracks in the chord at the weld toe of lengths up to 33% of the joint perimeter. The experimental tests on Grade 275 steel showed failure by ductile tearing and provided the first demonstration of the significant contribution of mode III loading in T joints with through thickness cracks under tension loading.

The UMIST work by Cheaitani[9] involved a similar combination of finite element analysis and model scale testing applied to 45^0 K joints under balanced axial loading with β values of 0.36, 0.53 and 0.79, with through thickness cracks at the crown of the tension brace of lengths up to 38% of the weld toe perimeter length. The experimental tests on Grade 275 material demonstrated that for this configuration, the effect of the presence of the crack at the tension brace weld toe was to undermine the support provided by the tension brace against buckling failure of the chord under the compression brace. Once this buckling failure started to occur, the severity of conditions at the crack tip increased substantially and tearing started to develop.

Both of the above investigations showed a progressive reduction in the ultimate strength of the cracked joints relative to the base line of an uncracked joint of the same geometry and loading configuration. The UMIST team recognised that there was likely to be a significant effect of absolute size on the possible incidence of **fracture failure as opposed to plastic collapse** and were concerned to provide simple recommendations which could be used as an input for fracture mechanics assessments. They therefore suggested that a safe assessment (lower bound) of the **plastic collapse strength** at a given value of crack length could be made by applying a reduction factor to the HSE characteristic strength formulae for the uncracked geometry but that fracture must be considered separately. This reduction factor for plastic collapse was recommended as follows:

$$\text{Reduction Factor RF} = \left[1 - \frac{\text{cracked area}}{(\text{intersection length} \times T)}\right]\left(\frac{1}{Q_{\beta}}\right)$$

As a result of the combined universities' research programmes, a recommended procedure for defect assessment in offshore structures was published by Burdekin and Cowling.[10]. A number of programmes have been carried out to extend and validate these initial findings. Finite element analysis programmes were carried out at UMIST by Al Laham[11] to extend the K joint work of Cheaitani to a β value close to 1.0 and to cover in plane and out of plane bending loading of K joints.

Work to investigate the significance of mixed mode loading was carried out by Yang[12] leading to advice on fracture mechanics treatments for taking account of mixed mode loading in tubular joints.

A major joint industry project was organised by TWI with larger scale experimental tests on Grade 355 steel and joint finite element analysis by TWI and UMIST[13]. The main part of this work was concerned with double T joints of a larger size than the UMIST model scale test carried out by Frodin and covering the cases of $\beta = 0.48$ and $\beta = 0.95$. This work covered through thickness cracks in the chord of 15% and 30% of the weld toe perimeter and also included examples of part thickness surface cracks. The associated finite element analysis covered loading in axial tension, axial compression and out of plane bending. Related work was also carried out by DNV[14] involving both finite element analysis and experimental testing on three DT joints with a β ratio of 0.43, one with a through thickness crack and the other two with surface cracks. Liverpool University[15] carried out three out of plane bending tests on DT joints with a β ratio of 0.53, two tests having through thickness cracks and one test a surface crack. An independent individual project had been completed by Skallerud et al[16] in 1994 involving two tests and associated finite element analysis on T joints with a β ratio of 0.4 and containing surface cracks.

Most of the experimental work described so far has been carried out on conventional structural steels of the Grade 275 or Grade 355 type. An extensive series of model scale tests was carried out by Nottingham University using models cast from a lead tin alloy[17]. Previous work using this technique on uncracked models had shown good agreement with conventional tests on steel models. The models used in the Nottingham work were small scale and the alloy showed ductile tearing behaviour so that the influence of fracture in these tests needs to be considered carefully.

A series of tests on six T and three Y joints in a high strength steel with a yield strength of 700 N/mm^2 has recently been completed at University College London[18]. These tests were carried out on joints with a chord diameter of 457 mm and had been subjected to prior fatigue testing. The cracks present were therefore representative of what might occur in service although in some cases more than one crack was present around the weld perimeter and the cracks were difficult to categorise in terms of their size.

All of the work described above has been concerned with the behaviour of brace to chord connections with cracks in the chord around the perimeter of the weld toe. As part of an investigation into the reliability of flooded member detection as a means of detecting members with through thickness cracks in bracing members, a major programme has been completed recently by UMIST and EQE which included finite element analysis studies on the behaviour of circumferential cracks in tubular members subject to axial tension[21]. This work found that the widely adopted solutions for the effects of cracks on ultimate strength of tubular members were not appropriate for use in conjunction with a fracture mechanics treatment and this is discussed further in the section of this report on circumferential cracks in tubular members.

A summary of all the experimental tests available on the ultimate strength of cracked tubular brace to chord joints is given in Table 1 and a summary of relevant finite element analysis work is given in Table 2. Reviews of the work in this area completed up to 1996 were included in papers to the 1996 OMAE Conference by Stacey, Sharp and Nichols[22,23]. The work reported in references 13 to 15 and 18 to 21 has been completed since those reviews. The present report includes all the later information and provides guidance on the overall question of assessment of the ultimate strength of cracked tubular joints.

2.1 Reduction factors applied to uncracked geometry characteristic strength

Although both the experimental test results and the finite element analysis predictions show significant scatter, Figures 1 and 2 are remarkable in showing the general trend for the strength of cracked tubular joints to follow the uncracked characteristic strength multiplied by an area reduction

factor. It is important to note that in Figure 1 the uncracked tension strength has been used as the basis for T and DT joints, whereas the uncracked compression strength has been used as the basis for K joints. The only results in Figure 1 which fall significantly below the HSE characteristic strength with reduction factor are those of Gibstein, Machida, Skallerud and some of the UCL high strength steel tests. It is vitally important to recognise that any prediction based on the strength of uncracked joints modified on an area reduction basis considers only **plastic collapse behaviour and takes no account of fracture.** The Gibstein and Machida tests are examples of failure by brittle fracture and clearly must be assessed taking this possibility into account. However, virtually all of the other tests showed ductile crack extension and tearing behaviour before final failure and the implications of this must also be taken into account. The high strength steel tests by UCL follow the same general pattern as those for the general structural steel tests as shown in Figure 1. It should be noted that the plastic collapse loads for the high strength steel would be higher than those for the general structural steels in proportion to the ratio of the yield strengths. Thus to achieve maximum failure loads in the experimental tests in proportion to the yield strengths, the fracture toughness of the high strength steel would also have to increase in the same proportion. Where such an increase in toughness is not available, the actual failure loads are more likely to be influenced by fracture rather than plastic collapse and are likely to fall below the simple area reduction correction factor prediction. This is likely to be the explanation for results falling below the area reduction line in Figure 1 including two of the high strength steel UCL tests. The results plotted in Figure 1 represent the initial crack length for the test and the maximum load reached, by which time the crack length would have increased considerably from the initial condition. It should also be noted that virtually all of the finite element analysis results shown in Figure 2 consider only a stationary crack and make no attempt to predict the effects of ductile tearing. Figure 2 shows both the HSE characteristic and HSE mean strengths with a linear reduction factor for cracked area. In a few cases, information is available from the experimental tests on the load at which ductile tearing is thought to have initiated and on the extent of ductile tearing at maximum load. Some examples of this are shown re plotted in Figure 3, showing the initiation conditions and the final failure conditions. It can be seen that in all cases the initiation conditions occurred at loads below the HSE characteristic strength modified by a reduction factor, but also in all cases the final failure condition was at loads higher than the modified HSE characteristic strength after allowing for the increase in crack length by tearing.

Clearly, although the use of the HSE characteristic strength multiplied by a reduction factor is a very useful basis for estimating the ultimate strength of tubular joints, it is not sufficient to use this without considering the possible effects of extension of the initial cracks by fracture. It should be noted particularly that although plastic collapse behaviour would be expected to be independent of size for geometrically similar samples, fracture behaviour is not independent of size. When model scale tests containing a crack of length a given proportion of the circumference are scaled up to a larger size, the absolute length of the crack is greater in the larger sized case and hence the crack tip conditions are more severe in the larger case at the same stress levels. Similarly with higher strength steels, a particular ratio of applied to yield strength will give a higher absolute stress level in the high strength steel case and for the same crack size, more severe crack tip conditions will be present in the high strength steel case.

More detailed consideration of fracture aspects requires the application of fracture mechanics methods as discussed in the Section 3.

2.2 Effects of chord end load on static strength of tubular joints

Some limited work has been carried out on the effect of chord end loads on the static strength of cracked tubular joints by Liverpool University and by UMIST. It is well known that there is a reduction in the static strength of uncracked tubular joints due to the presence of compressive loads in the chord and this is allowed for in the normal design procedures through the use of the Q_f parameter. The Liverpool work considered the effects of chord end compression loads on the strength of DT joints subject to out of plane loading and found reductions commensurate with those for the uncracked geometry[19]. The

UMIST work involved experimental and finite element analysis on 45^0 K joints under balanced axial loading with through-thickness cracks at the crown and compression loads in the chord[20]. This work found that the effect depended on how the net axial force in the chord from the forces in the brace was reacted. It should be noted that in any tests on K joints there is a net axial force component in the chord and that this effect will have been included in formulae for the strength of uncracked joints. It was found in the UMIST work that if the net axial force from the braces was reacted by an increase in the compressive force in the chord, then there was a reduction in the ultimate strength of the joints, but if the compressive reaction in the chord was kept constant as the net axial force from the braces was increased, there was little or no effect of the chord end load on the ultimate strength. The experimental work was primarily carried out keeping the reaction at the compressive end constant and this confirmed little or no reduction in ultimate strength. The finite element analyses explored both cases.

The UMIST finite element analysis results on 45^0 axially loaded K-joints results are illustrated in Figures 4 and 5 for uncracked and cracked joints respectively. The results for ultimate strength have been normalised by dividing by the static strength of the uncracked case with no additional chord end load. The inset diagram in Figure 4 shows a 45^0 K joint with forces P in each of the braces and forces RC at one end of the chord and RT at the other end. In an initial condition with no forces in the braces (P=0) any prior compression load in the chord gives RC=RT. As the forces P are increased a net axial force in the chord has to be reacted by a change in either RC or RT. If RC is kept constant then the reaction RT will have to move from compression towards tension to compensate for an increase in P and conversely if RT is kept constant then reaction RC will have to increase in compression to react the increased force P in the braces. The results in Figure 4 for the uncracked geometries show that when the reaction RC is kept constant there is little or no reduction in the ultimate strength represented by the brace load P for failure. On the other hand if the reaction RT is kept constant, with reaction RC increasing to balance the additional component of force in the chord from the brace loads, then there is a significant reduction in the ultimate strength for brace loads P. The results in Figure 5 for the cracked geometries show the same trends. The results are shown using the uncracked strength with no additional chord load as the normalising denominator so that the effect of the cracks for the two β ratios concerned can be seen with no additional chord load. There is very little further reduction due to chord end loads when RC is kept constant but significant further reductions occur if RT is kept constant.

In practice in a space frame offshore structure more complicated situations are likely to arise with multi planar tubular joints. However, it would appear that where a diagonal bracing member is in compression, at its bottom end it will cause an increase in the net compression in the chord (leg) below the joint which will be detrimental on ultimate strength. At the top end of a compression diagonal the effect will be to reduce the compression force in the chord (leg) below the joint so that this is not detrimental. Similarly at the top end of a diagonal bracing member in tension there will be an increase in the net compression in the chord below the joint which will be detrimental whereas at the bottom end of this member the effect would not be detrimental.

3. FRACTURE MECHANICS METHODOLOGY

In principle, it should be possible to assess the ultimate strength of cracked tubular joints using the fracture mechanics method of BS 7910[24]. This method involves the use of a failure assessment diagram which combines consideration of the failure modes of fracture and plastic collapse. The standard failure assessment diagram now current for BS7910 assessments is shown in Figure 6, although previous versions used in PD 6493 have had a slightly different form and basis.

To apply the BS 7910 methodology it is necessary to be able to estimate the fracture ratio K_r and the collapse ratio L_r. It should be noted that the fracture axis K_r uses the ratio of the **linear elastic** stress intensity factor to the fracture toughness whilst the collapse axis L_r uses the ratio of applied load to collapse load at the yield strength. Previous versions of the approach in PD 6493 used the ratio of the applied load to collapse load based on flow strength, termed S_r, with a diagram which terminated at S_r=1, whilst the present diagram allows for strain hardening above the yield strength by values of L_r greater than one.

For tubular joints the estimation of both the K_r and L_r parameters presents some difficulties. It is also necessary to know whether the BS 7910 failure assessment diagram is appropriate for the types of joint being assessed or whether some adjustments to the standard procedure are necessary. The situation is further complicated in some cases by the presence of mixed mode loading in some tubular joints. These different issues are considered in more detail in the following sections.

3.1 Estimation of K_r parameter (including mixed mode effects)

The only effective way of estimating stress intensity factors in complex geometries such as tubular joints is by means of carefully carried out finite element analyses. To obtain reasonable results it is important that careful attention is paid to the design of the finite element mesh and that modelling of the crack is carried out satisfactorily. A significant amount of work in this field has been carried out by UMIST, TWI, DNV, Swansea University and others using the ABAQUS program[25], often with automatic mesh generation systems such as PATRAN[26]. It must be recognised that for through-thickness cracks in the chord around the weld toe perimeter, there is a significant contribution to the total applied stress intensity factor from mode III loading. For part-thickness surface cracks the effect of mixed mode loading is much less significant, although there must be some contribution from mode II to the total K value. The method most commonly used to estimate stress intensity factors from finite element analysis is by determination of the J integral and converting this to equivalent K values. The J integral results obtained are those for all modes of loading combined and thus if there is mixed mode loading present, the effects will be automatically included in any determination of K from J[12].

For part-thickness surface defects, the most comprehensive results obtained are those from Bowness and Lee[27], although various approximate methods have been proposed. The basis of the simple models is to assume an equivalent plate T butt weld geometry under the action of the 'hot spot stress' due to the combination of membrane and bending stresses for the particular geometry of interest. This is summarised in the recommended procedure for defect assessment in offshore structures[10], for example at the deepest point of the crack as follows:

$$K_{primary(a)} = [M_{km(a)} M_{am(a)} M_{m(a)} F_{Wm} (1 - \Omega_{p(a)}) \sigma_{p(a)} + M_{kb(a)} M_{ab(a)} M_{b(a)} F_{Wb} \Omega_{p(a)} \sigma_{p(a)}] \sqrt{\pi.a}$$

and

$$K_{secondary(a)} = [Q_m M_{m(a)} + Q_b M_{b(a)}] \sqrt{\pi.a}$$

where the symbols have their usual meaning and are defined in reference 10, but $\sigma_{p(a)}$ is the hot spot stress for the uncracked geometry at the position corresponding to the deepest point of the crack and Ω is the degree of bending at this same position. The advantage of this formulation is that it can be applied to any situation for which there are parametric formulae available for hot spot stress

concentration factor, such as Efthymiou and Durkin[28], and for degree of bending, such as Connolly and Dover[29].

For through-thickness cracks around the weld toe in the chord, some results from UMIST finite element work are shown in Figure 7 in the form of non-dimensional K versus percentage of weld toe perimeter length cracked. The non-dimensional K is expressed as the ratio of the stress intensity factor to $\sigma_{HS}\sqrt{(\pi a)}$, where σ_{HS} is the hot spot stress in the uncracked structure **at the positions corresponding to the ends of the crack**, and 2a is the length of the through-thickness crack. It can be seen that for the cases considered with crack lengths up to 30% of the weld toe perimeter the non-dimensional K value is less than unity, but increasing as the crack length increases. As a safe estimate it has been recommended that the K value for through thickness cracks at the chord weld toe can be evaluated from:

$$K = \sigma_{HS}\sqrt{(\pi a)}$$

In general this will give an overestimate of the stress intensity factor for cracks up to 30% of the perimeter and hence lead to a safe assessment.

3.2 Estimation of L_r parameter

The L_r parameter is concerned with the interaction between plastic collapse and the effects of plasticity at the crack tip. It is usually defined as the ratio of the applied load to the load which would cause plastic collapse of the cracked geometry in a model made from elastic-perfectly plastic material.

The HSE equations are well established as a basis for predicting the strength of uncracked tubular joints and it is clear from the results shown in Figures 1 and 2 that the general trend for the effect of cracks on plastic collapse strength is to follow a linear reduction of area. The scatter in the results shown in Figures 1 and 2 is partly due to the intervention of fracture behaviour and partly inherent in the range of different geometries and materials considered.

The evidence from the results of finite element analysis of cracked geometries, presented in Figure 2, is that without ductile tearing effects, the HSE characteristic strength with reduction factor does represent a reasonable lower bound to the plastic collapse strength. The scatter in the finite element analysis results is of the same order as the scatter in experimental results and is attributed to effects of differences in geometry and material variations.

For the purposes of fracture mechanics assessments of tubular joints (brace to chord) it is recommended that the L_r parameter be calculated from the following expression:

$$L_r = \frac{P}{P_{ch}}.RF$$

$$\text{where Reduction Factor } RF = \left[1 - \frac{\text{cracked area}}{(\text{intersection length} \times T)}\right]\left(\frac{1}{Q_{ß}}\right)$$

However, this does not mean that the use of L_r calculated in this way will give results of failure assessments falling exactly on the standard assessment diagram, as the interaction with crack tip severity is also dependent on the geometry effects. It is necessary to consider the suitability of the standard diagram for particular applications.

3.3 Suitability of standard failure assessment diagram

As noted previously, the standard failure assessment diagram uses linear elastic values of the applied stress intensity factor to determine the fracture ratio K_r and allows for the effect of plasticity on the effective stress intensity factor by the shape of the assessment diagram itself. The standard diagram was originally determined for flat plate geometries and particular steels of the pressure

vessel/structural type. The relationship between the development of general plasticity and local crack tip conditions is somewhat dependent on both geometry and material properties.

A structure and material specific failure assessment diagram can be determined from the results of finite element analysis and a number of analyses of this kind have been carried out for tubular joints in the various programmes of work at UMIST[8,9,11,12], TWI[13], DNV[14] and by Kristiansen et al[30]. The procedure is to carry out a finite element analysis for the geometry and material of interest and to determine J integral values at identical load increments for elastic and elastic-plastic analyses. At any given load condition, the ratio $\sqrt{(J_e/J_{ep})}$ can be interpreted as equivalent to the fracture ratio K_r, on the assumption that fracture occurs at a critical value of the elastic-plastic J value, J_{ep}. Thus a graph of $\sqrt{(J_e/J_{ep})}$ against the load ratio L_r gives a structure specific version of the assessment diagram which can then be compared with the standard diagram in BS 7910. The results are highly dependent on the definition of L_r which is adopted. Some results from UMIST analyses of double T joints with β values of 0.48 and 0.95 under axial tension are shown in Figures 8 and 9 where the geometry specific failure assessment diagrams are compared with the standard level 2 assessment diagram from PD 6493. These diagrams were plotted using L_r derived from the HSE characteristic strength with area reduction factor. It can be seen that the geometry specific results for the through-thickness cases lie above and well outside the standard curve, so that using the standard curve for assessments would give very safe results. It can also be seen in Figure 9, however, that the results for the surface crack geometry, M215SC, fall very close to the standard curve. In a number of cases, geometry specific failure assessment diagrams have been found to fall just inside the standard assessment diagram for S_r values between about 0.7 and 1.0. This was also found to occur with part-thickness defects in the work by DNV[14], particularly for long surface defects. It is considered that this is probably due to the additional bending effects which occur for longer part thickness defects giving rise to increased crack tip severity.

The overall conclusion from this review is that to obtain best estimates of fracture mechanics assessments it is preferable to carry out a specific finite element analysis of the particular cracked geometry to estimate the maximum elastic plastic crack tip driving force and compare this directly with the fracture toughness. Approximate safe estimates of **fracture initiation** can be made using the BS7910 failure assessment diagram approach using the area reduction factor applied to the HSE characteristic strength for L_r and the estimation methods described above for the stress intensity factor. If the fracture toughness results are **brittle cleavage fracture** then the load at initiation should be taken as the load for the ultimate strength of the joint. **For any assessment involving materials showing cleavage fracture, the effects of residual stresses must be included as part of the crack tip driving force. For ductile tearing fracture the effects of residual stresses will be eliminated by yielding and plasticity and can be ignored after initiation.** Examples of assessments with ductile tearing fracture are discussed in the following section.

4 EXAMPLES OF APPLICATION OF FRACTURE MECHANICS TEARING ANALYSIS

Assessments involving tearing are currently not rigorous for crack extensions beyond a few millimetres. The experimental results shown in Figure 1 which involved ductile tearing showed tearing well beyond these limits. Nevertheless, it is possible to make some approximate estimates if some data are available on the tearing resistance of the materials concerned. Example analyses have been carried out on the experimental tests on DT joints carried out by TWI, for which the ductile tearing resistance data are shown in Figure 10. Although the experimental tearing data were limited to about 3 mm crack extension, the application to the tubular joints has assumed that the equations representing the R curve can be extrapolated to the amount of tearing in the tubular joints. This assumption cannot be justified theoretically but it will be seen that the results obtained are very reasonable.

The methodology put forward by UMIST previously involved the use of PD 6493 assessment diagrams and originally the Level 2 assessment diagram was used. This methodology has now been updated to be consistent with BS 7910 using the failure assessment diagrams based on the L_r parameter. To estimate the K_r (fracture parameter) the fracture toughness at a particular amount of crack extension J_{mat} has been converted to an equivalent stress intensity factor toughness by the following expression:

$$K_{mat} = \sqrt{\frac{E J_{mat}}{(1-\upsilon^2)}}$$

The stress intensity factor at the crack tip for the through-thickness crack cases has been estimated from the following expression:

$$K = C.\sigma_{HS}\sqrt{\pi.a}$$

where σ_{HS} is the hot spot stress at the position around the perimeter corresponding to the crack tips, 2a is the full length of the through thickness crack, and C is a coefficient derived from the previous FE work at UMIST shown in Figure 7. In the present analyses C has been taken as 1 which would be expected to overestimate the applied K value and give conservative (safe) predictions. For the part-thickness case, the K value was estimated from the hot spot stress and plate K solutions until the crack had torn through the thickness and then the through-thickness approach was used. The hot spot stress was determined by interpolation between the saddle and crown values given by the Efthymiou and Durkin parametric equations. The degree of bending was determined from the UCL equations derived during the Defect Assessment Programme.

The L_r parameter has been estimated from the HSE characteristic strength equation for the uncracked geometry in question under axial loading, modified by an area reduction factor based on the net cross section around the weld toe perimeter.

The calculations have been carried out to determine the stress in the brace and hence the brace load for initiation of fracture from the initial crack length in the tubular joint tests, T1/1, T1/2, T2/1 and T2/3. In each case an arbitrary increase in crack length has then been assumed, and the calculations repeated to determine the load at which the combination of K_r and L_r lie on the standard assessment diagram for the increased toughness associated with moving along the assumed R curve by an amount corresponding to the assumed increase in crack length. These calculations were carried out by a simple spreadsheet program and then repeated iteratively for further assumed increments in crack extension. In the case of the high β joints of the T2 series, the calculations were carried out both removing the Q_β effect and without removing it. The effect of these analyses is that the failure assessment point moves progressively along the FAD towards the plastic collapse end of the diagram. What is happening effectively is that as the crack tears the remaining area reduces until eventually a plastic collapse

condition is reached and the load starts to reduce. This is shown in Figures 11 to 16 for the different cases of through-thickness cracks considered and in Figure 17 for the surface crack case T1/4. The loads at different crack extension increments are marked at different positions around the various FADs. Although not shown on the diagrams it is remarkable that the amount of ductile crack extension at which the maximum load behaviour was observed was very close to that found in the actual experiments on the tubular joints despite the assumptions made. In all cases the predicted maximum loads from these tearing analyses were less than the actual failure loads and a comparison of these is shown in Figure 18.

It can be seen from Figure 18 that the predicted maximum loads are always less than the experimental loads. It should be borne in mind however that the failure assessment diagrams used to predict the tearing behaviour have used an L_r parameter based on the HSE characteristic strength and hence safe predictions are to be expected.

5. CIRCUMFERENTIAL CRACKS IN TUBULAR MEMBERS

A major programme of work has been carried out at UMIST on effects of circumferential cracks in tubes as part of a study of the reliability of flooded member detection. This work included determination of stress intensity factors (SIFs) and plastic collapse solutions for a range of cracked geometries for surface cracks with a/t ratios of 0.8 and greater and length to circumference ratios (2c/l) of up to 0.4[21]. Existing published solutions such as those in BS7910 are restricted to a/t ratios up to 0.8. A subsequent programme has carried out an experimental investigation of the effect of deep surface and through thickness circumferential cracks on the ultimate strength of plain tubes with tests carried out by UMIST and UCL and analysis and reporting by UMIST[31].

5.1 Finite element Analysis Results for Stress Intensity Factors for Circumferential Cracks

(a) SIFs for tubes with surface cracks with a/t $\geq$0.8

Examples of the results for stress intensity factors for semi-elliptical surface cracks in tubes with a γ (R/t) ratio of 17, with crack depth to thickness ratios 0.8, 0.95 and 0.99, and with crack length to tube circumference ratios of 0.2 and 0.4 are shown in Figures 19 and 20. The results are expressed for different positions around the crack front (angle ϕ) in terms of the non-dimensional stress intensity factor K'_I given by:

$$K'_I = \frac{\sqrt{E.J}}{\sigma\sqrt{\pi.a}}$$

For all the tubes' cases analysed, K' values are smallest at the free surface, with the lower a/t ratio cases having slightly higher values at this point than the higher ones. In addition, these values are quite small compared to the maximum values located at the deepest point of the crack; the deeper the crack, the higher the K' values. Comparison of the results shown in Figures 19 and 20 also shows that K' values increase with the length to circumference ratios 2c/l.

(b) SIFs for tubes with through-thickness cracks

Similar methods were used to determine tables of the K' values versus the distance along the crack front (with respect to the outside surface of the tube) were generated. In this case the normalisation was carried out with respect to the crack length c, i.e. $K' = K/(\sigma\sqrt{(\pi.c)})$. Examples of the resulting curves are given in Figures 21 to 23. The SIFs curves show that the thinner the tube the higher the SIFs, and the maximum values of K' are located at or near the inner surface of the tube for relatively long cracks (2c/l>0.20). It also observed that the SIFs values increase with crack length ratio (2c/l). This is expected because apart from the reducing area available for the directly applied tensile loading, the induced bending stresses increase with the crack length.

5.2 Failure Assessment Diagrams for Circumferential Cracks in Tubes

The principles of deriving geometry specific failure assessment diagrams by use of finite element analysis were described in Section 3.3. The same methods were used to derive FADs for circumferential surface and through thickness cracks in plain tubes.

(a) FADs for surface cracks

The results of finite element analyses to determine failure assessment diagrams for circumferential surface cracks with a/t=0.8 and a/t=0.95 are shown in Figure 24. In this figure the L_r parameter has been determined using the recommendations from BS7910 based on the Kastner solutions. It can be seen that all of the geometry specific FADs lie above and well outside the standard BS 7910 FAD. The use of the standard FAD as the boundary to determine the acceptability of cracks would be highly

conservative as assessment points which lie outside the standard curve would be judged unacceptable whereas if they were inside the geometry specific curves they would in fact be safe. This is because the Kastner solution for part thickness surface cracks is based on a local collapse criterion for the remaining ligament whereas the finite element analysis solution gives the real effect of increasing plasticity at the crack tip contained by the surrounding material.

(b) FADs for through thickness cracks

The results of finite element analyses to determine failure assessment diagrams for circumferential through thickness cracks are shown in Figure 25. In this case it can be seen that the geometry specific FAD curves fall inside the standard BS 7910 FAD over values of L_r up to 1. The trend is that longer crack lengths give results further inside the standard FAD. For these cases use of the standard BS7910 FAD would be unsafe because assessment points lying inside the standard FAD would be deemed safe whereas if they lay outside the geometry specific FAD they would in fact be unsafe.

5.3 Modified values of L_r for use with standard FAD for circumferential cracks

Recommendations have been made in the UMIST work[21] for adjustments to be made to the calculations of L_r to enable more accurate assessments to be made using the standard BS 7910 FAD. For each of the geometry specific FAD curves determined from the finite element analysis, at each level of the ratio of applied remote stress to yield stress, the appropriate value of L_r was determined to correct the geometry specific FAD to lie on top of the standard FAD. The correction factors were then expressed in the form of equations to give L_r in terms of the ratio of applied to yield stress for the specific crack and tube geometries analysed. These equations are given in Appendix A. Examples of the results are shown in Figure 26 for surface defects with a/t=0.8 and in Figure 27 for through thickness defects.

5.4 Experimental tests of circumferential cracks in tubes

A series of experimental tests has been carried out by UMIST with assistance from University College London to validate the findings from the UMIST analytical programme referred to above. The results are reported in full in reference 32. A total of 16 tests were carried out by UMIST on small scale tubes of diameter 139 mm x 5 mm thickness and four tests were carried out by UCL on large scale tubes of diameter 500 mm x 20 mm thickness. The tests included through thickness cracks of lengths 110 mm to 350 mm in the small scale tests and 180 mm or 720 mm in the large scale tests. The surface crack tests were on tubes with initial crack depths 0.8 of the thickness x various lengths over the same range as the through thickness crack cases. In all cases crack extension occurred by ductile tearing, although in some of the deep surface crack cases an unstable burst of ductile fracture occurred as the crack broke through to a full thickness condition of the same crack length.

The results of plotting these test results on a failure assessment diagram basis are shown in Figures 28 and 29. Figure 28 shows the results when based on the BS 7910 approach with L_r values calculated using the Kastner equations. Figure 29 shows the results using the UMIST method for correcting L_r values as described in Section 5.3. It can be seen that the BS 7910 approach represented by Figure 28 gives substantially more scatter with some results for through thickness cracks unsafe and with considerable conservatism for the surface crack cases. The scatter is substantially reduced when the UMIST correction factors are applied as shown in Figure 29. The results in Figure 29 falling marginally inside the standard FAD are believed to be due to the effect of the end attachments used in the tests having a reduced bending resistance compared to the inherent bending strength of the tubes themselves.

6. CONCLUDING REMARKS

A review of the existing experimental evidence available on the static strength of cracked tubular brace to chord joints has shown that there is a broad trend for the strength to be reduced from that of the uncracked geometry in proportion to the reduction in cross sectional area. However, it is essential to consider separately the possible modes of failure by plastic collapse and by fracture. Furthermore it is essential to differentiate between brittle fracture and ductile tearing fracture.

The plastic collapse strength of cracked tubular joints can be estimated reasonably by using the HSE design formulae for uncracked joints modified by an area reduction factor based on the ratio of the area of the crack to that of the perimeter of the joint. A safe estimate can be obtained by using the HSE characteristic strength equations and removing any strengthening benefit from the Q_β term as this may well be countered by the presence of the crack.

To obtain estimates of the fracture strength of the cracked joint or member it is necessary to carry out a fracture mechanics analysis. The most accurate way to achieve this is to carry out a geometry specific finite element analysis, including modelling of the crack itself. It is clear form the work reported in the literature that this approach is now feasible using 3D elastic plastic finite element methods. Since the resources for this may not always be available, and it may in any event be desirable to carry out some scoping calculations before embarking on expensive and complex finite element analyses, some methods for carrying out approximate analyses have been outlined and example calculations presented in the report. These approximate methods are based on the use of the BS7910 defect assessment procedures and include recommendations for determining the stress intensity factor ratio K_r and the collapse load ratio L_r.

A procedure for carrying out a tearing analysis for cracks in tubular joints has been described and a series of model calculations carried out for joints which had been part of an experimental programme. Although the procedure has been extrapolated beyond the region supported by basic theory, the results show good agreement with experiments for the amount of tearing experienced and give safe predictions of maximum load.

An important set of analytical results is presented for the case of circumferential cracks in plane tubular members where the results suggest that the standard procedures of BS 7910 may not be appropriate.

7. REFERENCES

1. American Petroleum Institute, Recommended Practice for planning, designing and constructing fixed offshore platforms, RP2A 20th edition, API,Washington, USA,1993
2. Health and Safety Executive Offshore Installations: Guidance on design, construction and certification, HSE, London, UK, Fourth Edition, 3rd amendment, 1995 (now withdrawn).
3. Dier A., and Lalani M., New code formulations for tubular joint static strength, Eighth International Symposium on tubular structures, Singapore, August 1998.
4. Kurobane Y., Makino Y., and Sagawa M., Low cycle fatigue research on tubular joints, IIW Doc XV-291-70, International Institute of Welding, 1970.
5. Gibstein M.B., Fatigue strength of welded tubular joints tested at DNV Laboratories, International Conference on Steel in Marine Structures, Paper ST 8.5, Paris, October 1981.
6. Gibstein M.B., and Moe E.T., Brittle fracture risks in tubular joints, Proc. Fifth International OMAE Conference, Vol II, pp 144-152, ASME 1986.
7. Machida S., Hagiwara Y., and Kajimoto K., Evaluation of brittle fracture strength of tubular joints of offshore structures, Proc. Sixth International OMAE Conference, Vol III, pp 231-237, ASME 1987.
8. Burdekin F.M. and Frodin J.G., Ultimate failure of tubular connections, Final Report Project DA709, Department of Civil and Structural Engineering, UMIST, November 1987.
9. Cheaitani M.J. and Burdekin F.M., Ultimate strength of cracked tubular joints, Tubular Structures VI, Grundy Holgate and Wong (eds), Rotterdam.
10. Burdekin F.M. and Cowling M.J., Defect assessment in offshore structures – a procedure, CMPT Publication 100/98, ISBN 1 870553 330.
11. Al Laham S., and Burdekin F.M., The ultimate strength of cracked tubular K-joints, Department of Civil and Structural Engineering, UMIST, Final Report to UK Health and Safety Executive, 1995.
12. Burdekin F.M. and Yang G.J., Failure assessment diagrams for mixed mode loading and cracked tubular joints, Advances in fracture research, ICF9, Vol 1, pp27-37, Sydney, Australia, 1997.
13. Hadley I., Dyer A.P., Booth G.S., Cheaitani M.J., Burdekin F.M. and Yang G.J., Static strength of cracked tubular joints: new data and models, Proc. OMAE Lisbon 1998, ASME 1998.
14. Klasen B., Wastberg S., and Moe E.T., Failure assessment diagram method for tubular joints, DNV Technical Report 96-3012, Det Norske Veritas, Norway, 1996.
15. Ting K.T. and Moffat D.G., Static strength of cracked DT tubular joints under out of plane bending moment, Department of Engineering Report A/170/95, University of Liverpool, 1995.
16. Skallerud B., Eide O.I., and Berge S., Ultimate strength of cracked tubular joints: comparison between numerical simulations and experiments, Proc. Seventh BOSS Conference Boston 1994 , Volume III, pp 241-260, July 1994.
17. Hyde T.H., Fessler H. and Khalid Y.A., Effects of cracks at one saddle on the static strength of T, Y, and YT tubular joints, Department of Mechanical Engineering, University of Nottingham, Final Report to UK Health and Safety Executive, 1994.
18. Talei-Faz B., Dover W.D., and Brennan F.P., Static strength of cracked high strength steel tubular joints, UCL NDE Centre, February 1999.
19. Kang C.T., Moffatt D.G., and Mistry J., Ultimate strength of a DT tubular joint subjected to chord compression and brace out-of-plane bending, J. Strain Analysis, 1998.
20. Burdekin F.M. and Xu W.G., Effects of chord axial compression on the ultimate strengths of cracked K-joints, Department of Civil and Structural Engineering UMIST, Final report to Health and Safety Executive, March 1999.
21. Burdekin F.M., Thurlbeck S.D., Sanderson D., Kiwanuka F. and Hamour W., Joint industry project on the reliability of flooded member detection as a tool for assurance of integrity, Final Report, EQE Ltd. and UMIST, 1999.

22. Stacey A., Sharp J.V., and Nichols N.W., The influence of cracks on the static strength of tubular joints, Proc. OMAE Florence 1996, Volume III, Materials Engineering, ASME 1996.
23. Stacey A., Sharp J.V., and Nichols N.W., Static strength assessment of cracked tubular joints, Proc. OMAE Florence 1996, Volume III, Materials Engineering, ASME 1996.
24. BS7910: Guide on methods for assessing the acceptability of flaws in fusion welded Structures, BSI, 1999.
25. Hibbit, Karlsson & Sorensen, Inc: ABAQUS/Standard User's Manuals (Vol.1-3), Ver.5.8, 1998.
26. PDA Engineering, PATRAN Division: PATRAN, Version 6.0, California, 1996.
27. Bowness D., and Lee M.M.K., Weld toe magnification factors for semi-elliptical cracks in T-butt joints, Offshore Technology Report, OTO 99 014, Health and Safety Executive, London, 1999.
28. Efthymiou M. and Durkin S., Stress concentration in T/Y and gap/overlap K joints, BOSS Conference, Delft 1985.
29. Connolly M.P., Hellier A.K., Dover W.D., and Sutomo J.,A parametric study of the ratio of bending to membrane stress in tubular Y and T joints, International Journal of Fatigue, Vol 12, No 1, pp 3-11, ISSN 0142-1123
30. Kristiansen, N.O., Noad C.E. and Turner C.E., An R6 FAD analysis of a cracked T-joint under brace tension, Proc. 11th OMAE Conference, Vol III, pp 299-306, ASME 1992.
31. Burdekin F.M., Experimental validation of the ultimate strength of brace members with circumferential cracks, UMIST Final Report to Health and Safety Executive, October 2001

Table 1 Summary of experimental test data on ultimate strength of cracked tubular joints

Investigation	No. of tests	Joint Type	Loading	D (mm)	T (mm)	b	t	g	Type of crack	% Crack Area
Gibstein	7	T	Axial Tension	508	16	0.48		15.9	TT	80
	1	Y	Axial Tension	508	16	0.48		15.9	TT	80
	4	T	Axial Tension	578	30	0.52		9.63	Surface	0.3,1.4,10.2,
Kurobane	1	K	Balanced axial	102	3.2	0.42		16.0	TT	30
	4	K	Balanced axial	102	3.1	0.42		16.3	Surface	0,1.3,3.2,11
UMIST (Frodin)	4	DT	Axial Tension	142	5	0.34		14.2	TT	12,23,33
	4	DT	Axial Tension	141	5	0.54		14.9	TT	10,21,32
	4	DT	Axial Tension	139	5	0.82		13.9	TT	10,21,32
UMIST (Cheaitani)	3	K	Balanced axial	168	6	0.36	0.82	14.0	TT	28,36,38
	3	K	Balanced axial	114	3.6	0.53	0.89	15.8	TT	27,36,36
	3	K	Balanced axial	76	3.2	0.79	1.0	11.9	TT	24,35,35
TWI	3	DT	Axial Tension	572	19	0.48	0.5	15.0	TT	0,15,30
	1	DT	Axial Tension	572	19	0.48	0.5	15.0	Surface	15
	3	DT	Axial Tension	572	20	0.95	1.0	14.3	TT	0,15,30
Machida	2	T	Axial Tension	580	40	0.62		7.25	Surface	3
Skallerud	2	T	Axial Tension	508	20	0.4		12.7	Surface	20,40
Liverpool	2	DT	OPB	169	7.4	0.53	0.74	11.4	TT	0, 28
	1	DT	OPB	169	7.4	0.53	0.74	11.4	Surface	14
SINTEF	1	T	IPB	914	32	0.5	0.5	14.3	TT	47
DNV	1	DT	Axial Tension	572	25	0.43	0.8	11.4	TT	45
	2	DT	Axial Tension	572	25	0.43	0.8	11.4	Surface	7, 17
Nottingham	12	T	Axial Tension			0.33,0.5,0.67	0.67,0.96,1.15	18.4,10.2	TT	11,20,25,33
	9	T	OPB			0.33,0.5,0.67	0.67,0.961.15	18.4,10.2	TT	11,20,25,33
	1	T	Axial Comp.			0.5	0.96	18.4	TT	20
	3	T	Axial Tension			0.5	0.96	18.4,10.2	Surface	4,8
	3	T	OPB			0.5	0.96	18.4, 10.2	Surface	4, 8, 9.4,
	2	Y	Axial Tension			0.5	0.96	18.4	TT	20
	2	Y	OPB			0.5	0.96	18.4	TT	20
	3	YT	Balanced axial			0.5	0.96	18.4	TT	20
	2	YT	Balanced axial			0.5	0.96	18.4	Surface	8
UCL	6	T	Axial Tension	457	16	0.71	1.0	14.3	TT	16,18,20,46
	3	Y	Axial Tension	457	16	0.71	1.0	14.3	TT	45,70

Table 2 Summary of finite element analysis data on ultimate strength of cracked tubular joints

Investigation	No. of analyses	Joint Type	Loading	D (mm)	T (mm)	b	t	g	Type of crack	% Crack Area
UMIST (Frodin)	4	DT	Axial Tension	142	5	0.34		14.2	TT	0,12,23,33
	4	DT	Axial Tension	141	5	0.54		14.9	TT	0,10,21,32
	4	DT	Axial Tension	139	5	0.82		13.9	TT	0,10,21,32
UMIST (Cheaitani)	3	K	Balanced axial	168	6	0.36	0.82	14.0	TT	28,36,38
	3	K	Balanced axial	114	3.6	0.53	0.89	15.8	TT	27,36,36
	3	K	Balanced axial	76	3.2	0.79	1.0	11.9	TT	24,35,35
UMIST/TWI	3	DT	Axial Tension	572	19	0.48	0.5	15.0	TT	0,15,30
	1	DT	Axial Tension	572	19	0.48	0.5	15.0	Surface	15
	3	DT	Axial Compress	572	19	0.48	0.5	15.0	TT	0,15,30
	3	DT	OPB	572	19	0.48	0.5	15.0	TT	0,15,30
	3	DT	Axial Tension	572	20	0.95	1.0	14.3	TT	0,15,30
Skallerud	3	DT	Axial Compress	572	20	0.95	1.0	14.3	TT	0,15,30
Liverpool	3	DT	OPB	572	20	0.95	1.0	14.3	TT	0,15,30
	2	T	Axial Tension	508	20	0.4		12.7	Surface	20,40
Sintef	2	DT	OPB	169	7.4	0.53	0.74	11.4	TT	0, 28
DNV	1	DT	OPB	169	7.4	0.53	0.74	11.4	Surface	14
	1	T	IPB	914	32	0.5	0.5	14.3	TT	47
	1	DT	Axial Tension	572	25	0.43	0.8	11.4	TT	45
	2	DT	Axial Tension	572	25	0.43	0.8	11.4	Surface	7, 17

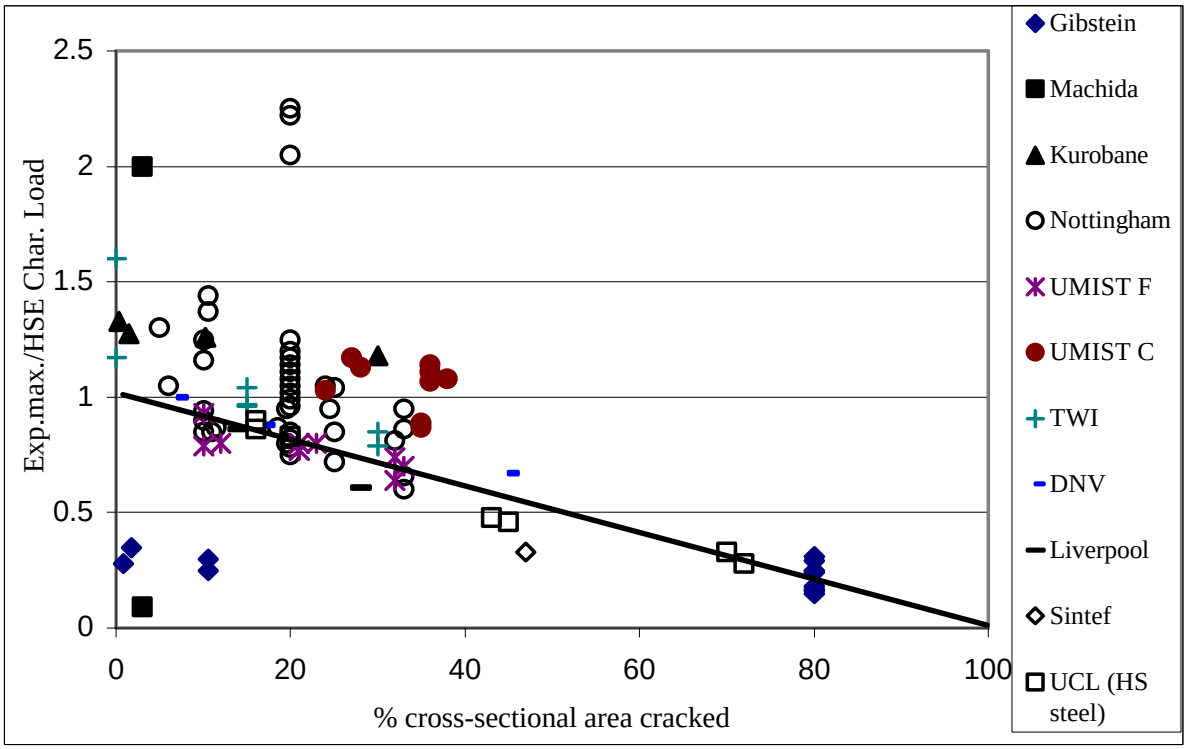

Figure 1 Results of experimental tests on ultimate strength of cracked tubular joints

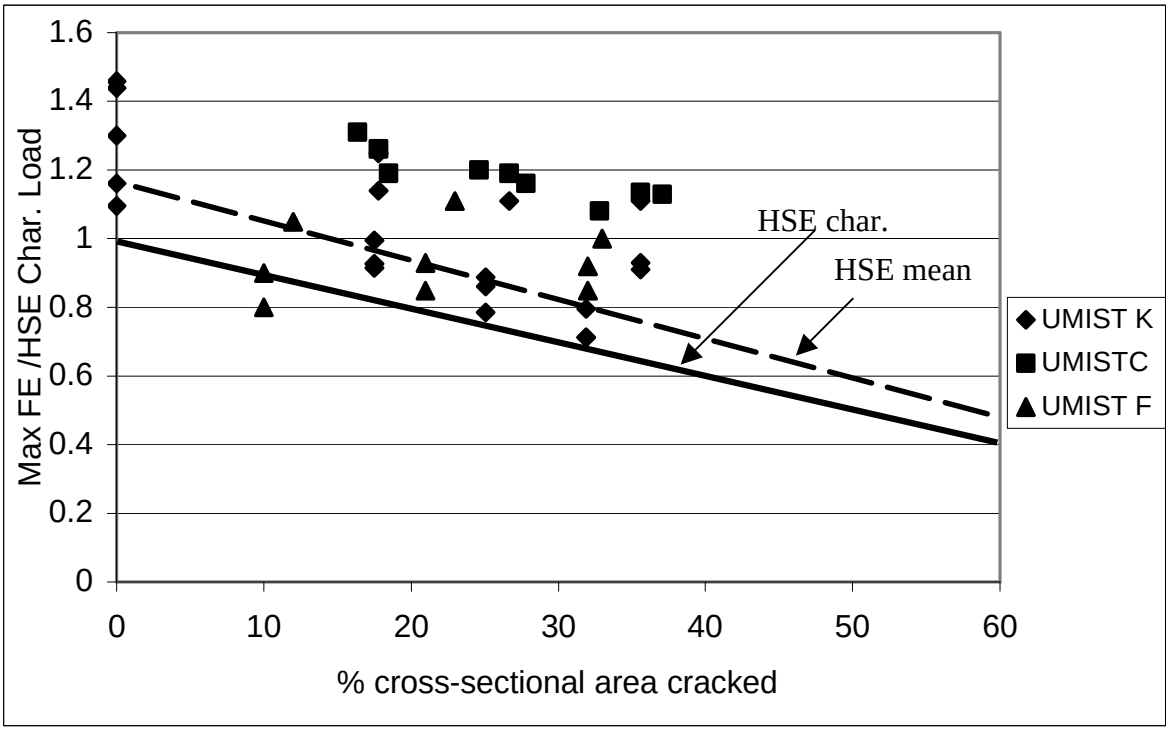

Figure 2 Results of finite element analyses for estimated maximum load for cracked tubular joint analyses.

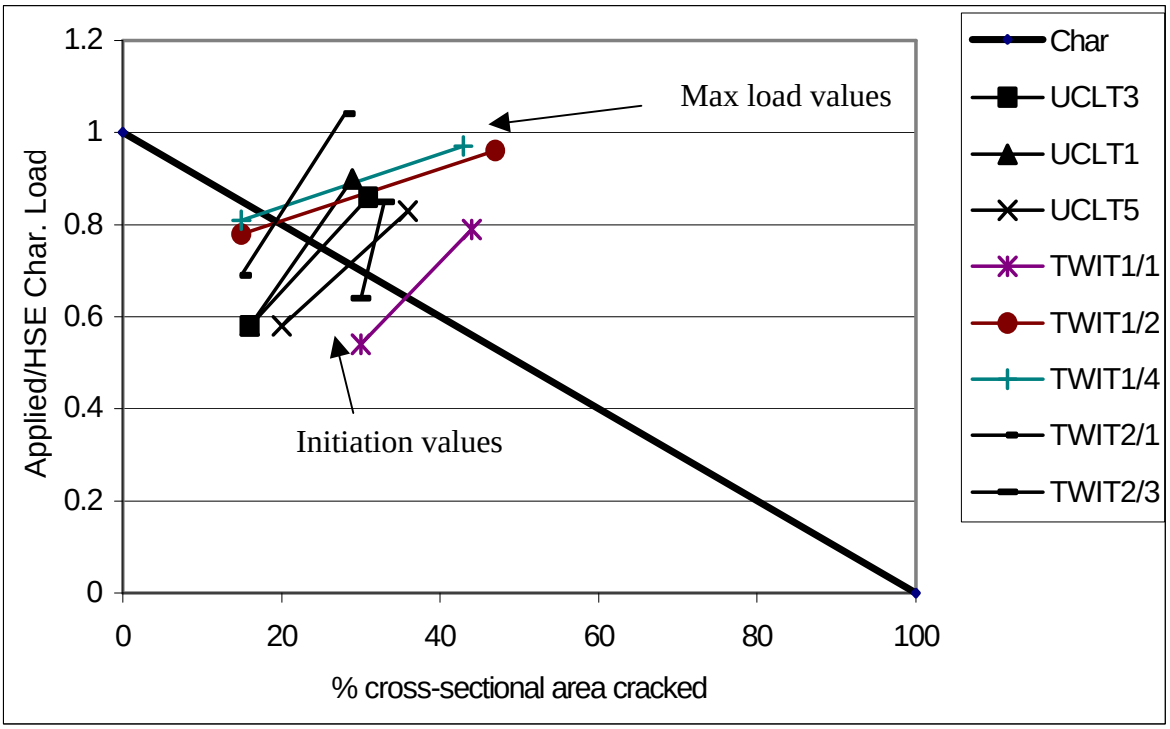

Figure 3 Estimates of conditions for initiation and final failure after tearing in some tubular joint tests.

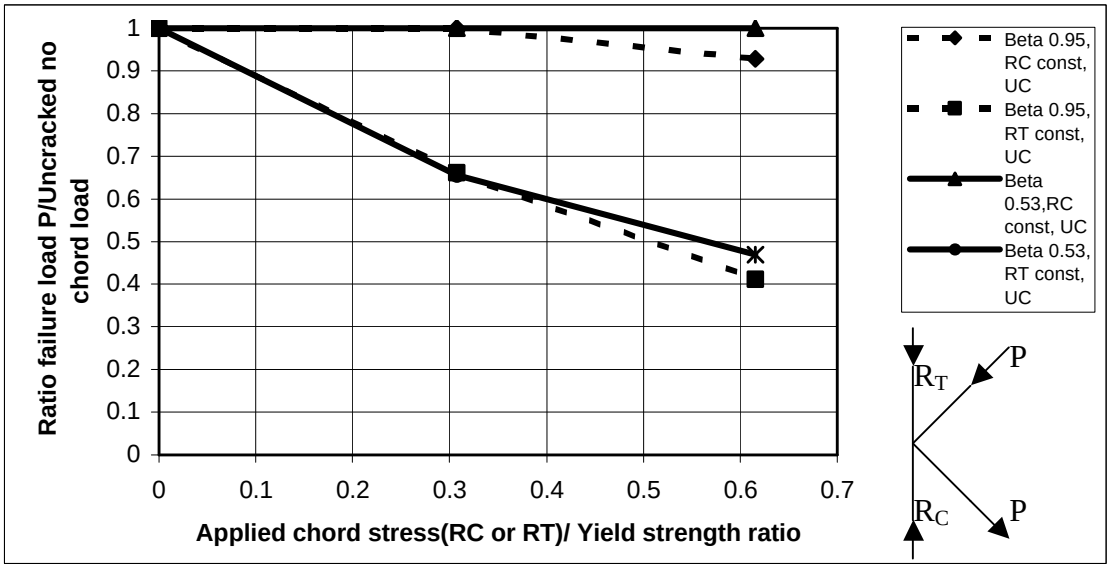

Figure 4 Effects of chord end load on ultimate strength of uncracked K-joints from finite element analyses

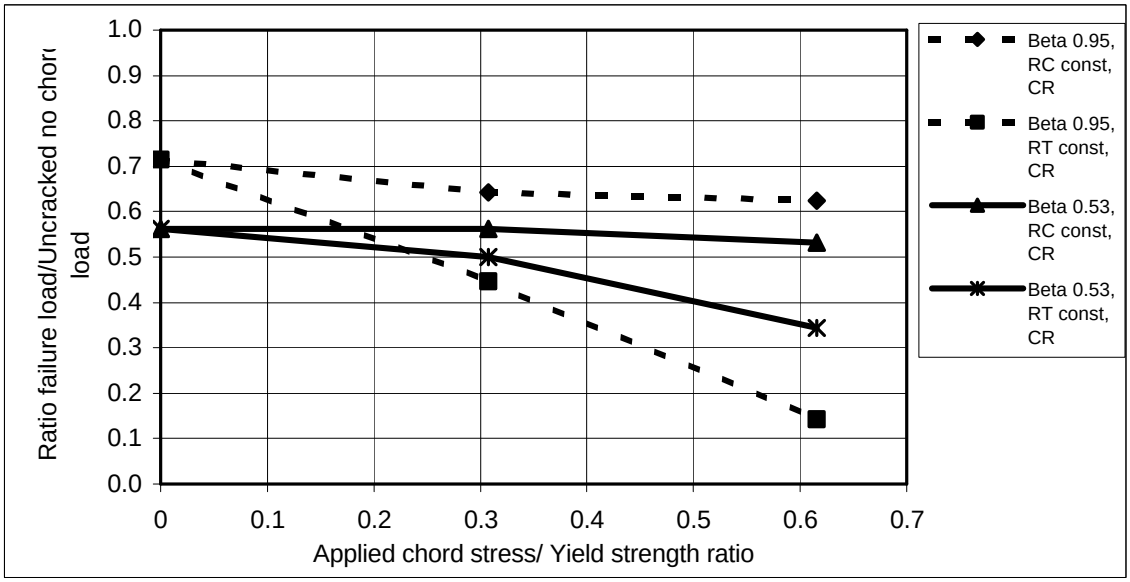

Figure 5 Effects of chord end load on ultimate strength of cracked K-joints from finite element analyses

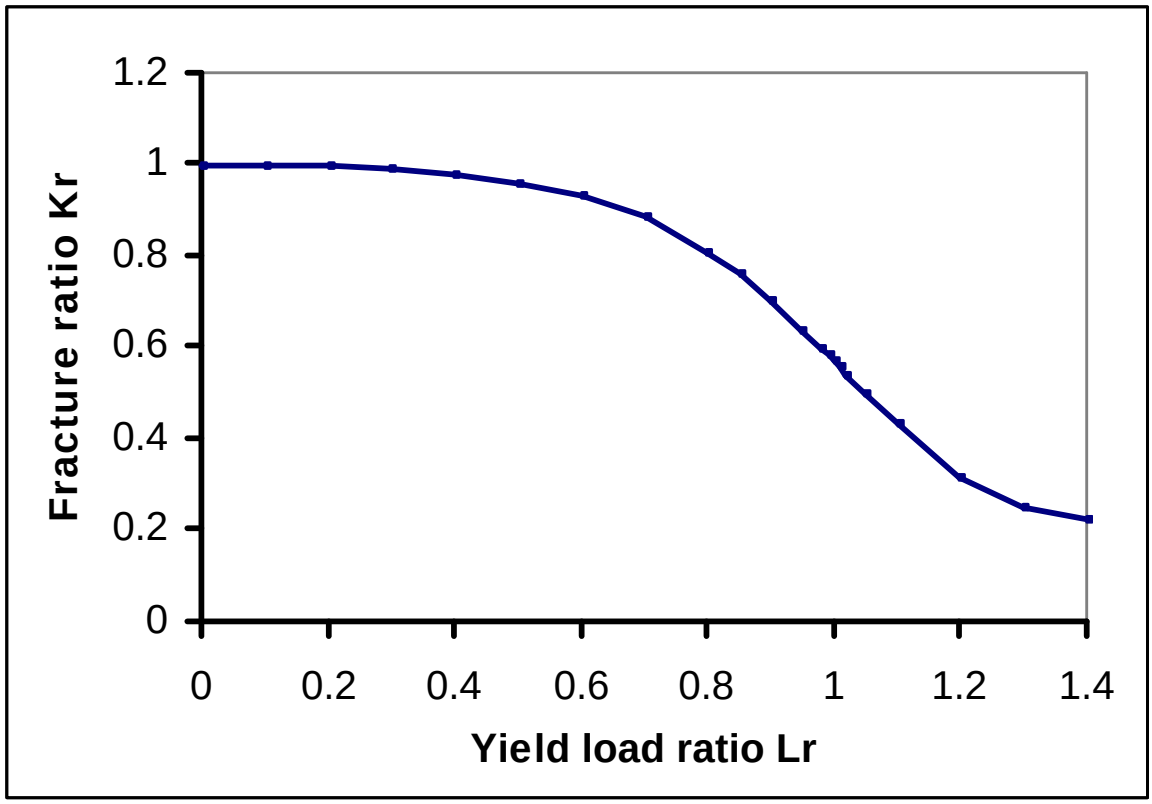

Figure 6 The BS7910/R6 Failure Assessment Diagram

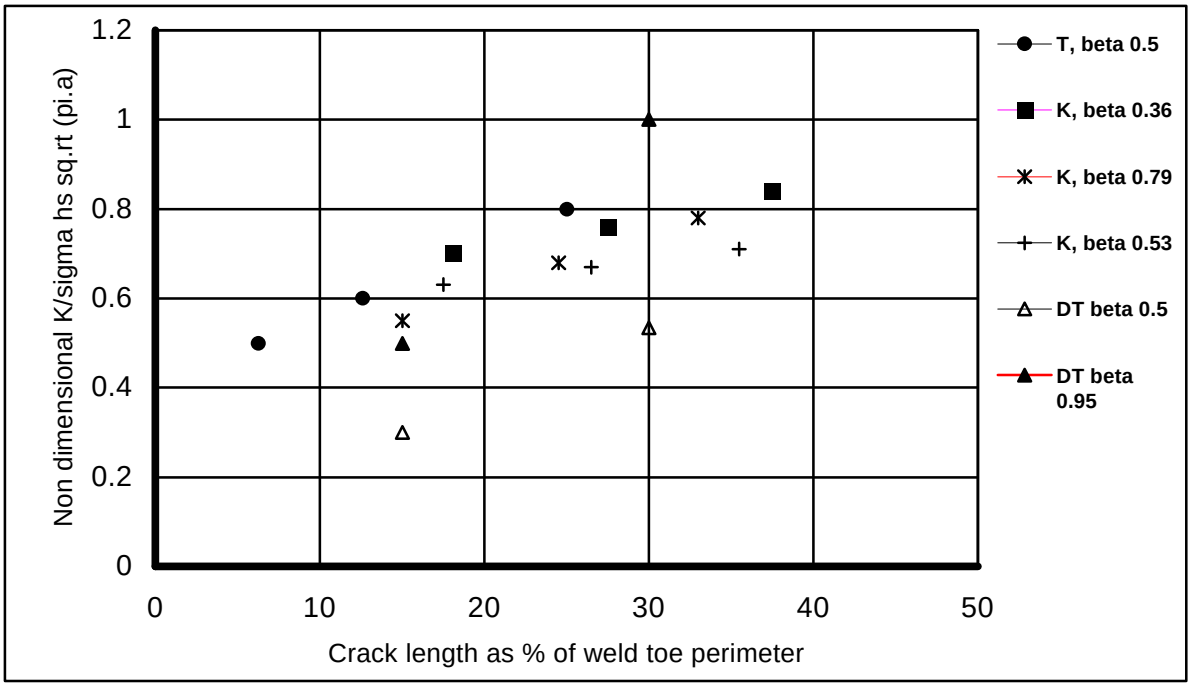

Figure 7 Estimates of non dimensional stress intensity factor for cracks at chord weld toe T, DT and K tubular joints from finite element analysis.

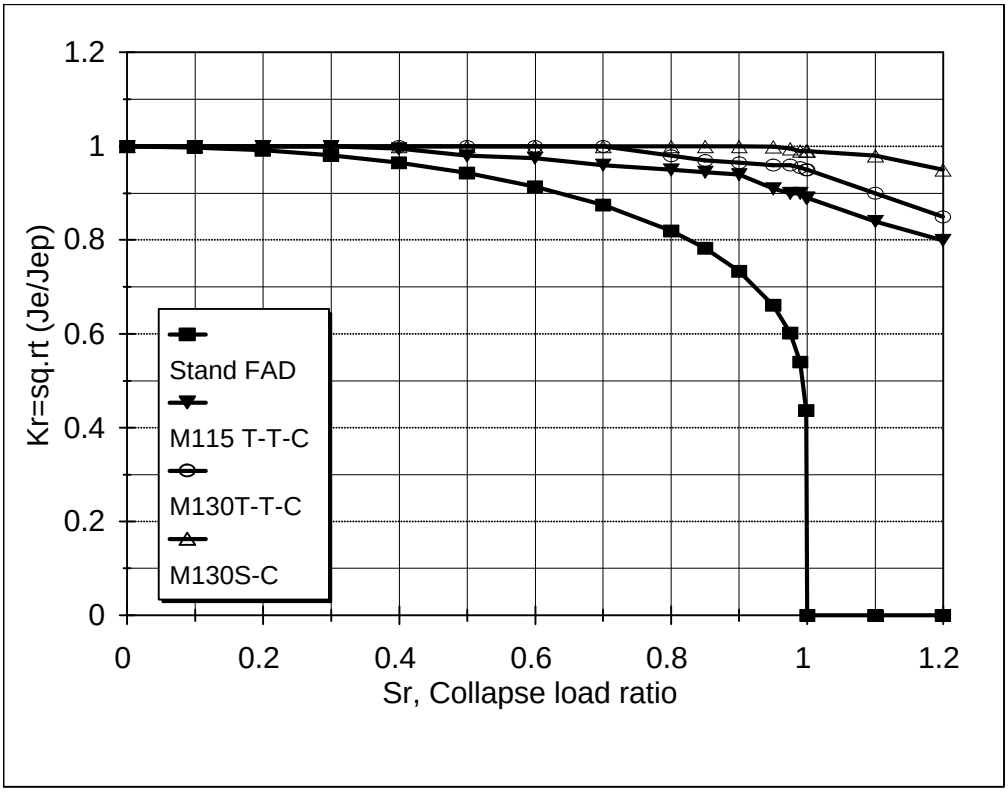

Figure 8 Specific failure assessment diagram from FE analysis of DT joint (β=0.48) under tension.

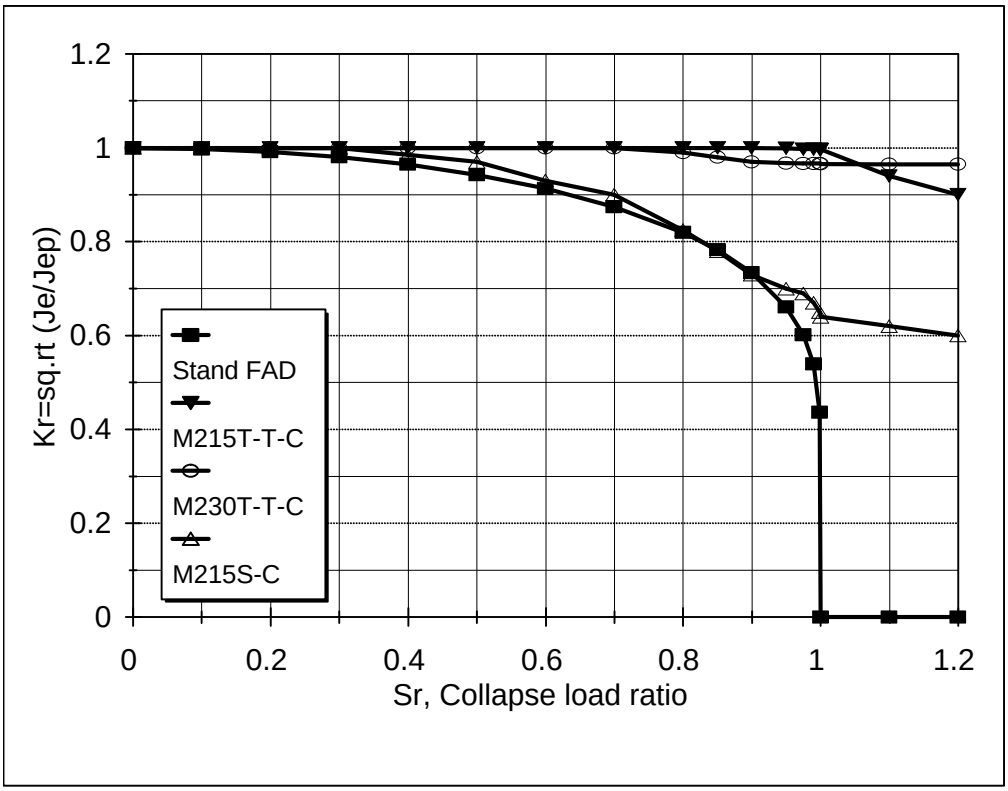

Figure 9 Specific failure assessment diagram from FE analysis of DT joint (β=0.95) under tension.

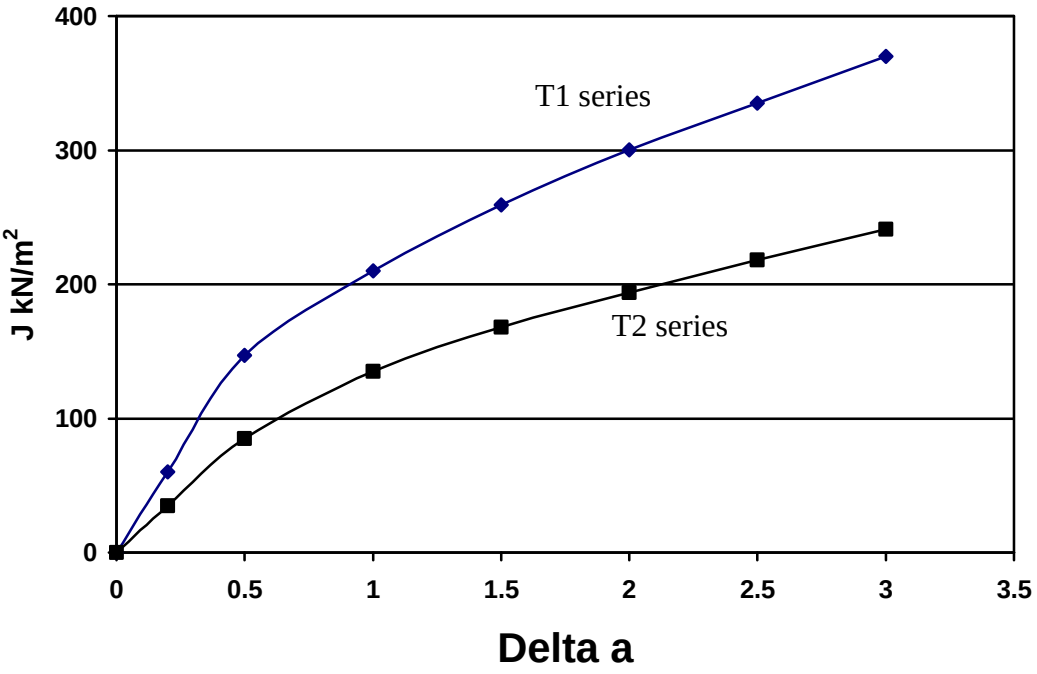

Figure 10 R-curve data for TWI tests

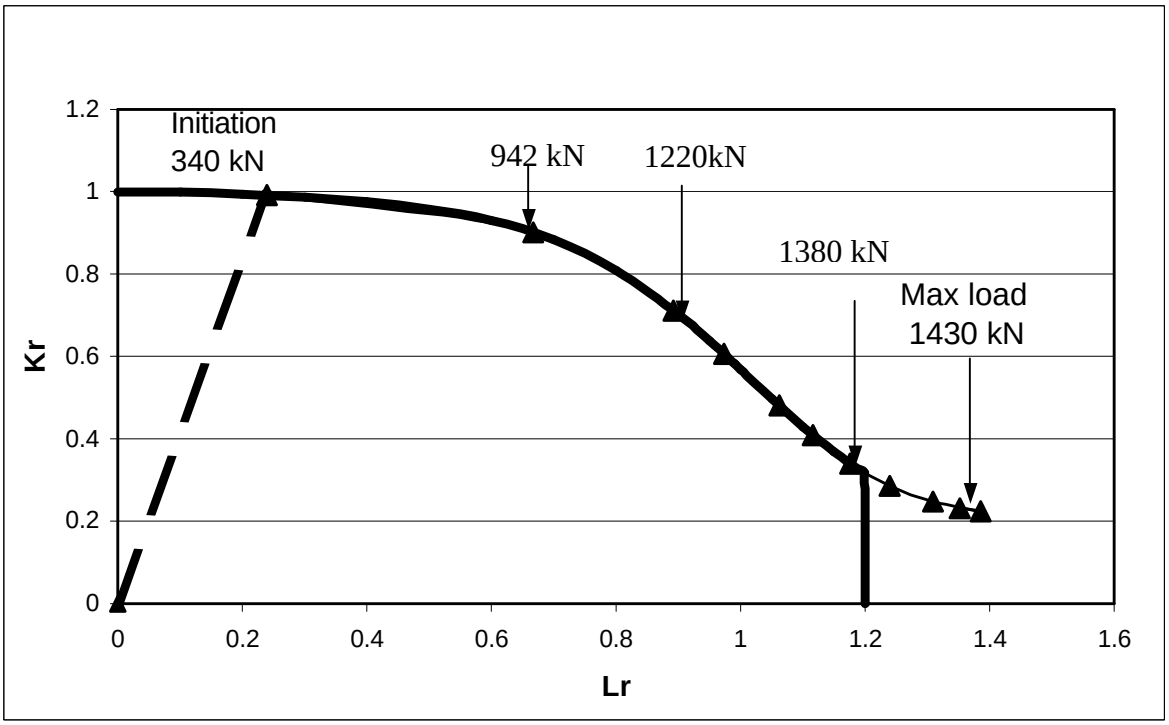

Figure 11 BS7910/R6 Failure Assessment Diagram for tearing in T1/1

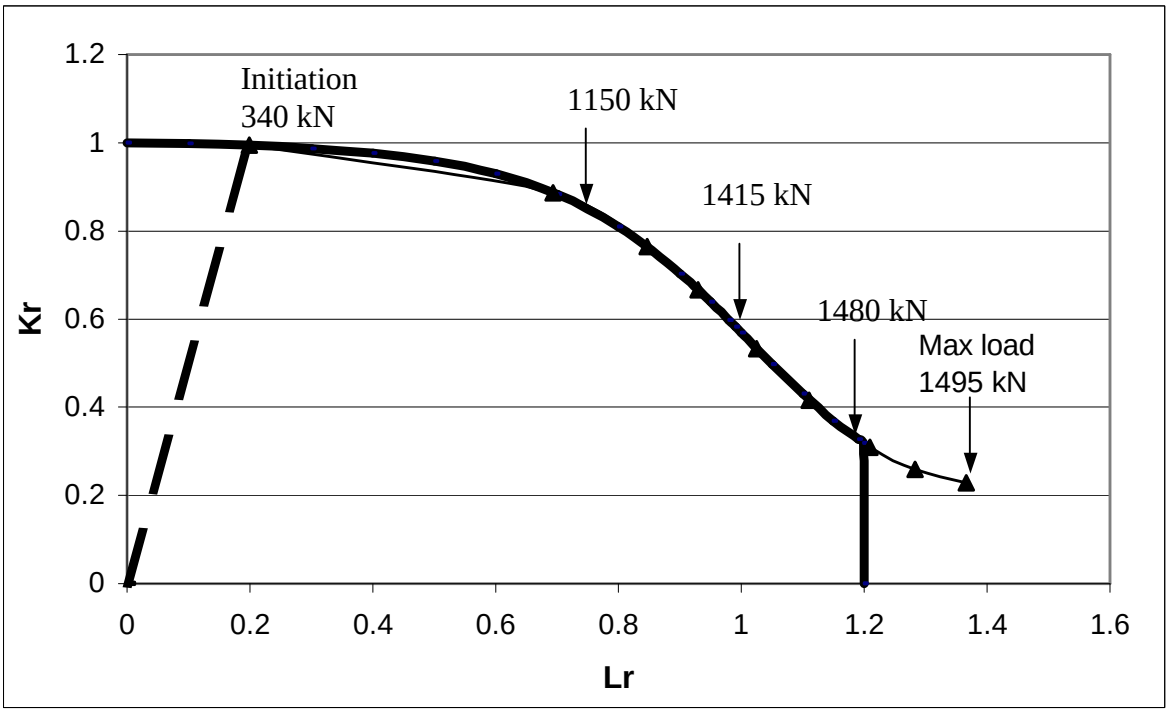

Figure 12 BS7910/R6 Failure Assessment Diagram for tearing in T1/2

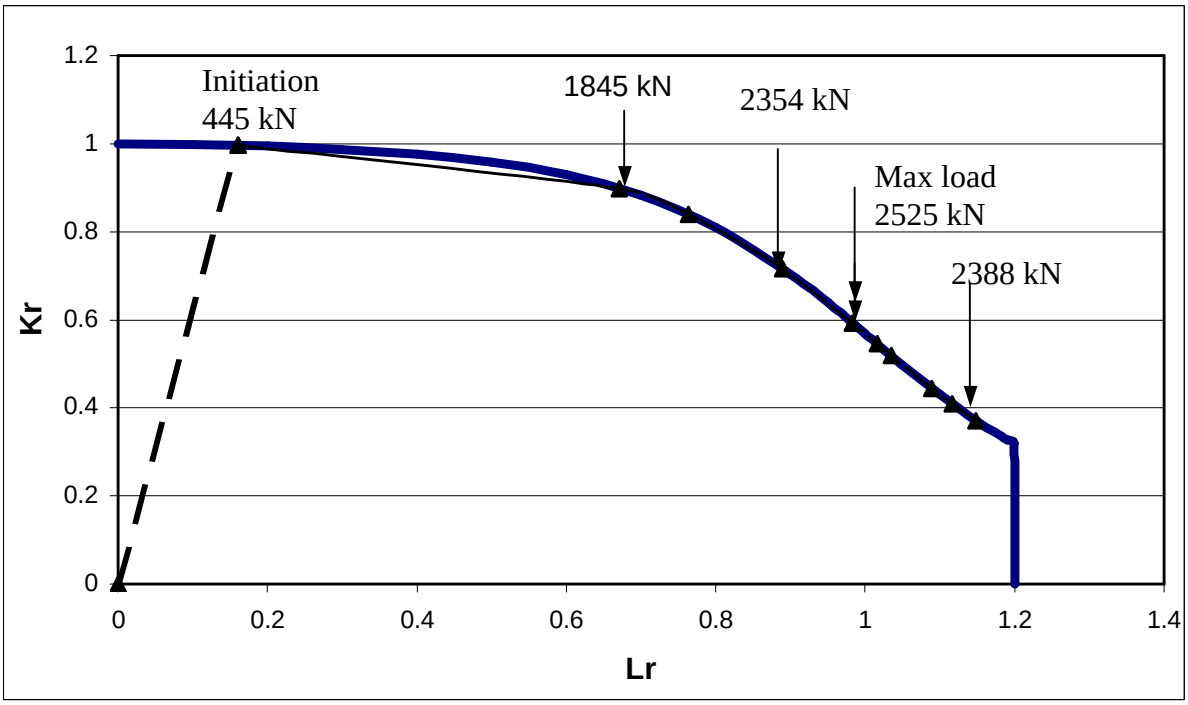

Figure 13 BS7910/R6 Failure Assessment Diagram for tearing in T2/1 with Q_β effect taken out

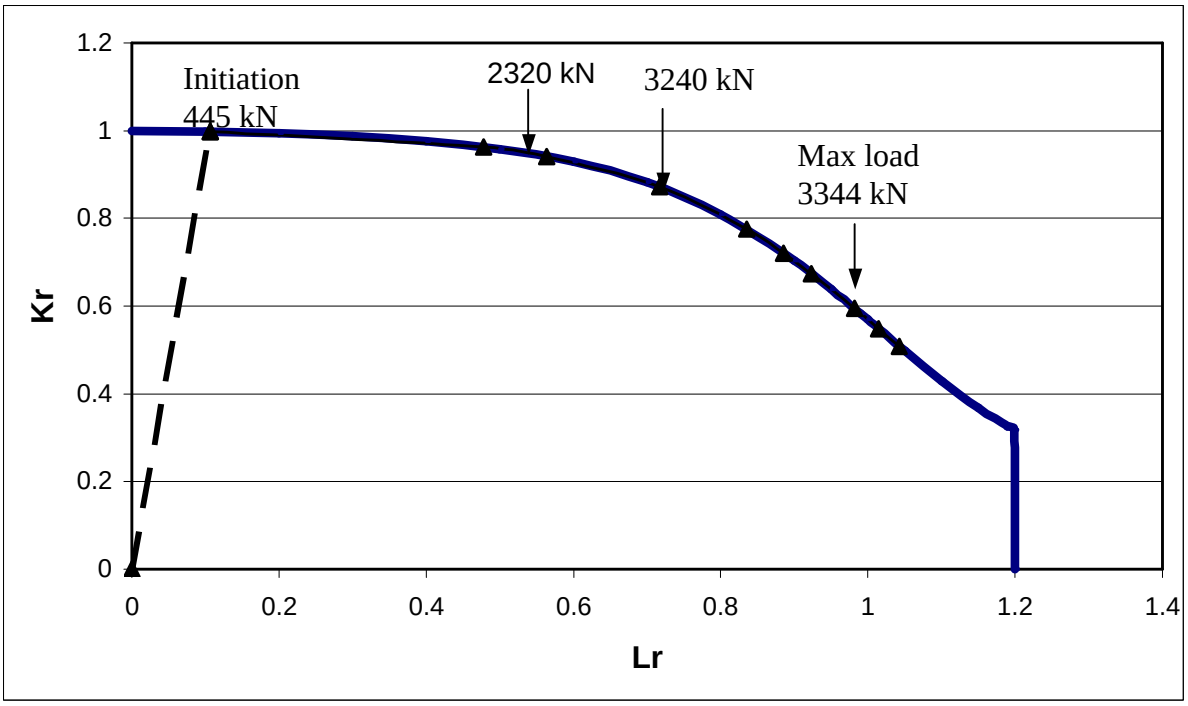

Figure 14 BS7910/R6 Failure Assessment Diagram for tearing in T2/1 with Q_β effect left in

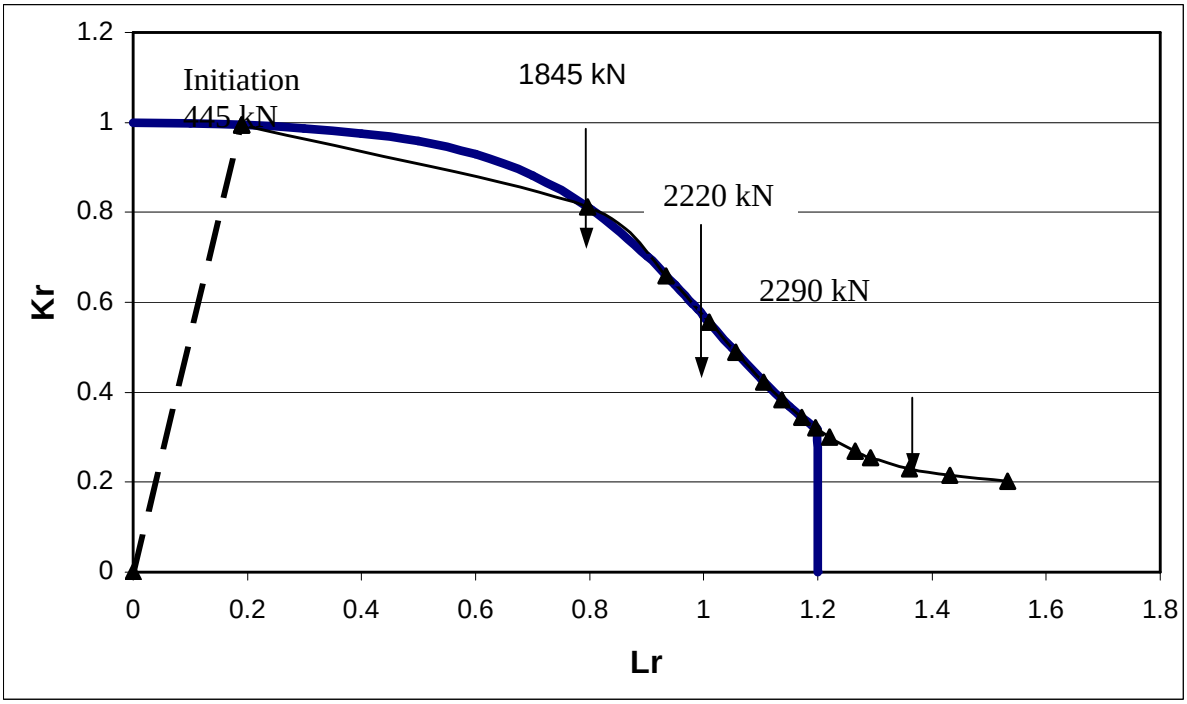

Figure 15 BS7910/R6 Failure Assessment Diagram for tearing in T2/3 with Q_β effect taken out

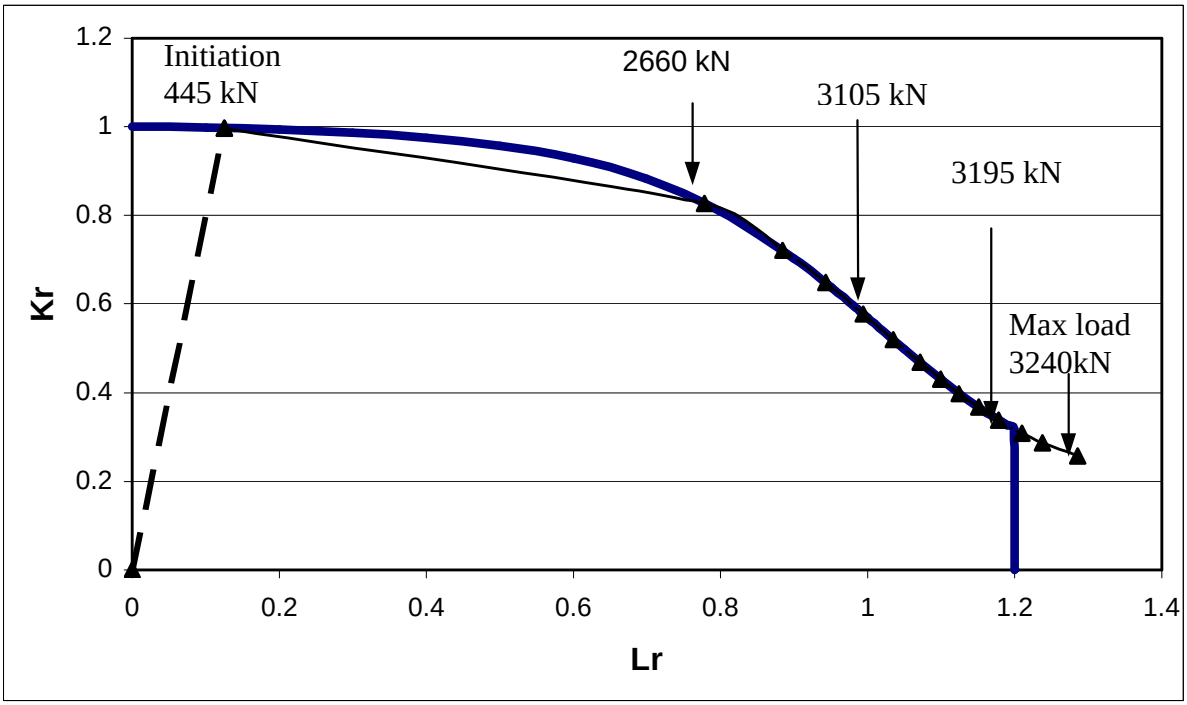

Figure 16 BS7910/R6 Failure Assessment Diagram for tearing in T2/3 with Q_β effect left in

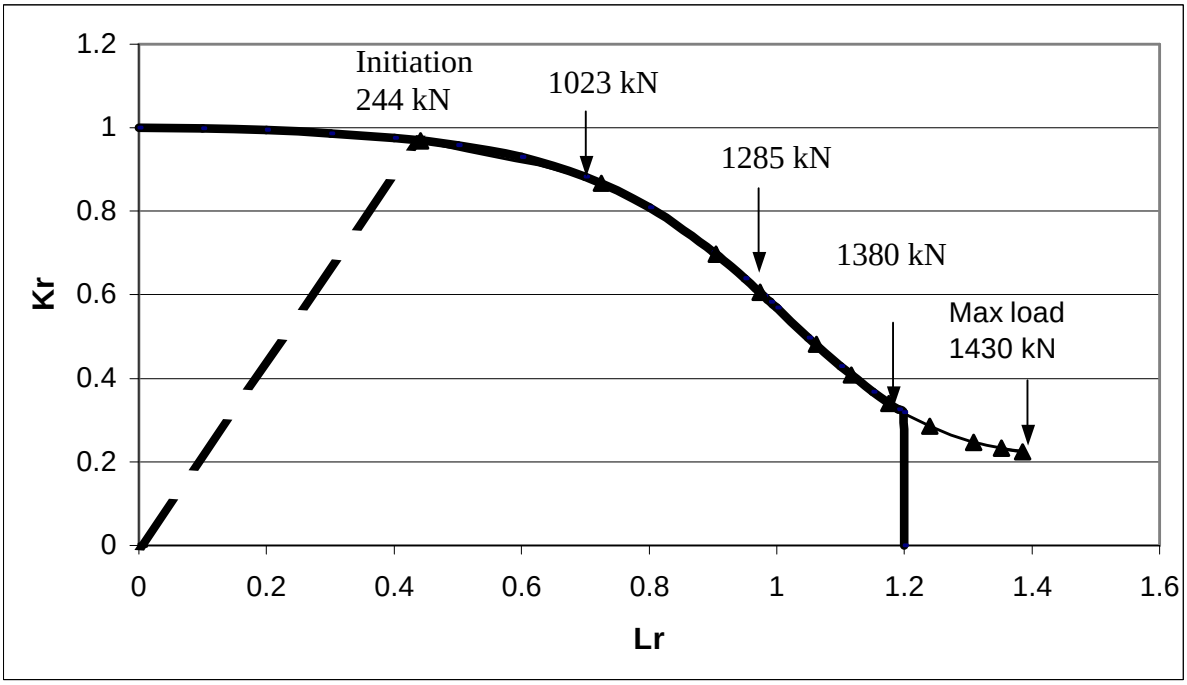

Figure 17 BS7910/R6 Failure Assessment Diagram for tearing in T1/4

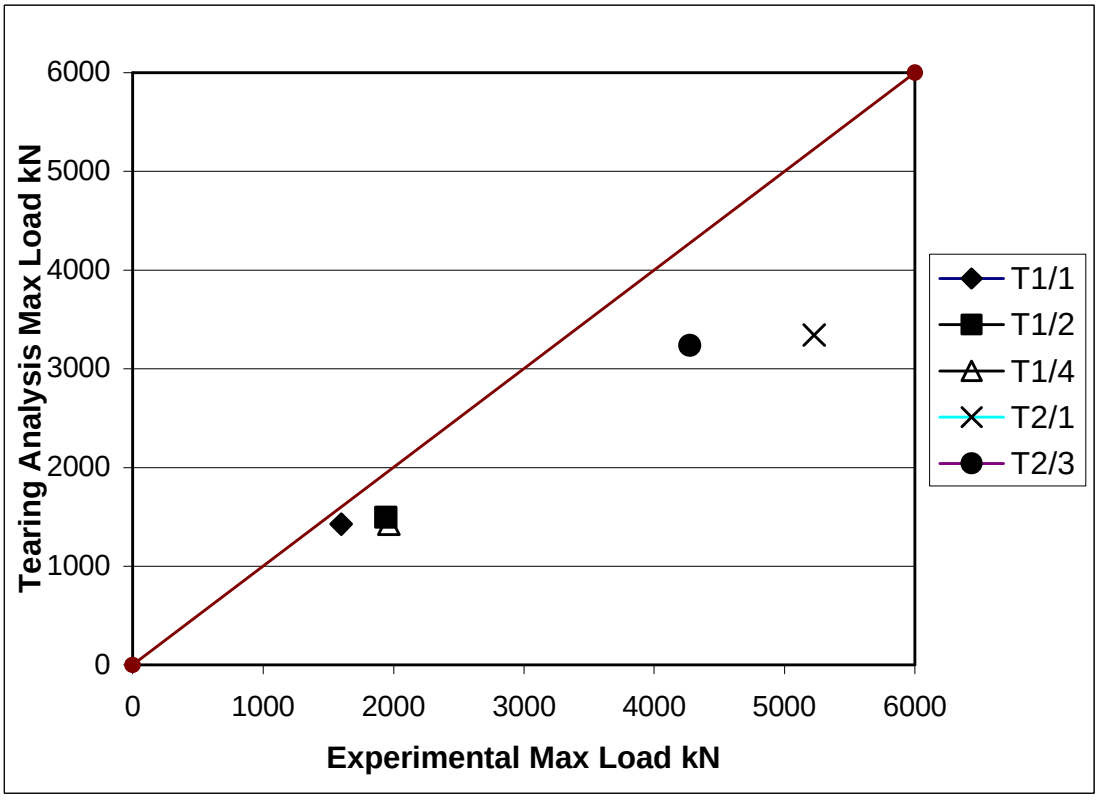

Figure 18 Comparison of tearing analysis maximum loads with experiment

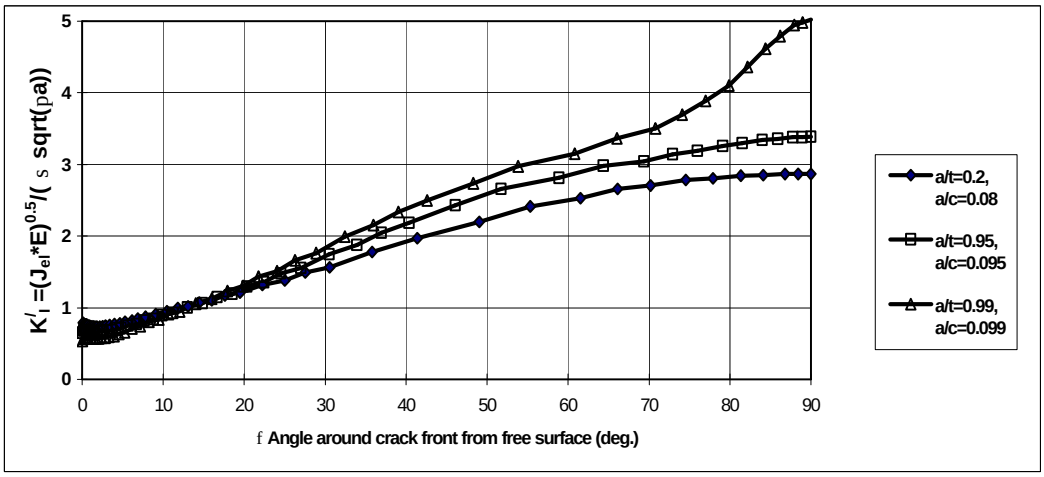

Figure 19 Normalised SIFs for semi-elliptical surface cracks in tubes with 2c/l = 0.2, R/t =17

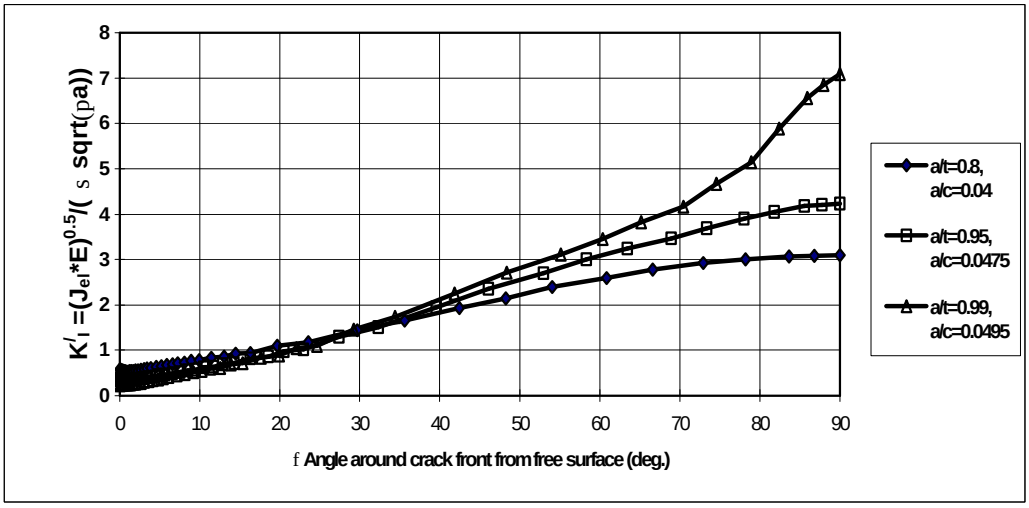

Figure 20 Normalised SIFs for semi-elliptical surface cracks in tubes with 2c/l=0.4, R/t=17

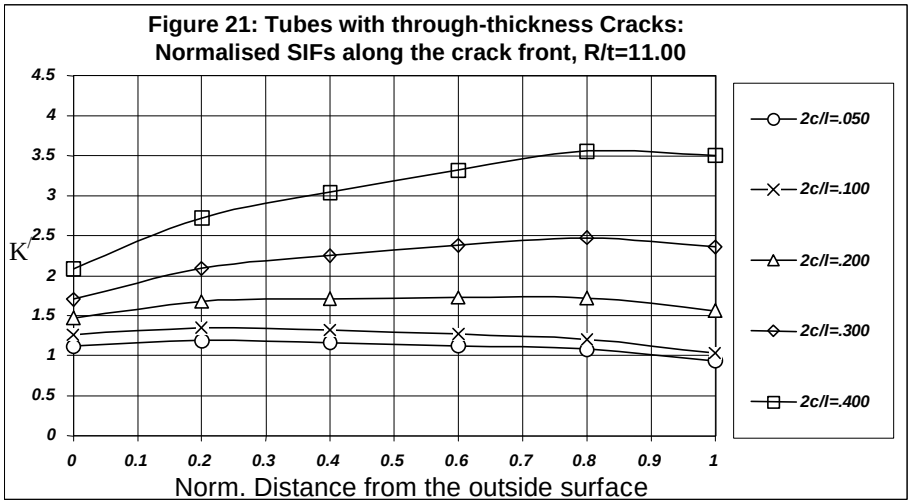
Figure 21: Tubes with through-thickness Cracks:
Normalised SIFs along the crack front, R/t=11.00
K/
4.5
4
3.5
3
2.5
2
1.5
1
0.5
0
0
0.1
0.2
0.3
0.4
0.5
0.6
0.7
0.8
0.9
1
2c/l=.050
2c/l=.100
2c/l=.200
2c/l=.300
2c/l=.400
Norm. Distance from the outside surface

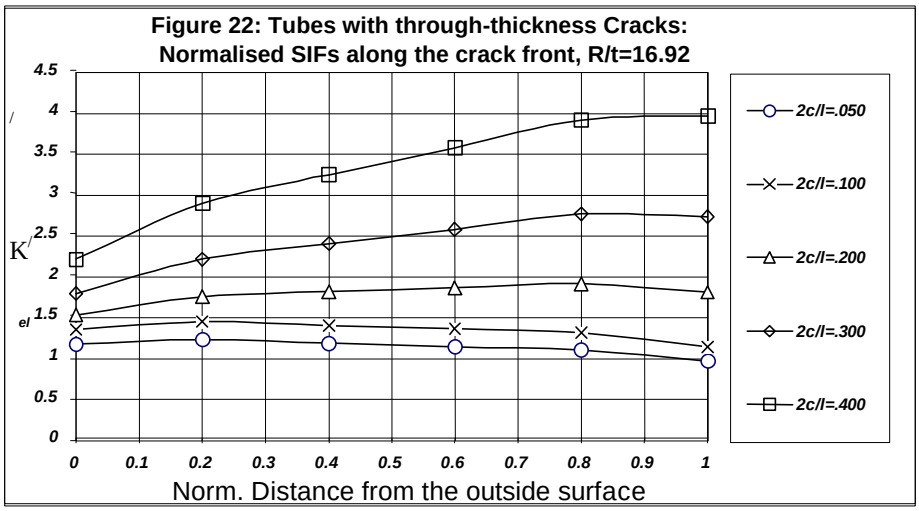
Figure 22: Tubes with through-thickness Cracks:
Normalised SIFs along the crack front, R/t=16.92
K/el
4.5
4
3.5
3
2.5
2
1.5
1
0.5
0
0
0.1
0.2
0.3
0.4
0.5
0.6
0.7
0.8
0.9
1
2c/l=.050
2c/l=.100
2c/l=.200
2c/l=.300
2c/l=.400
Norm. Distance from the outside surface

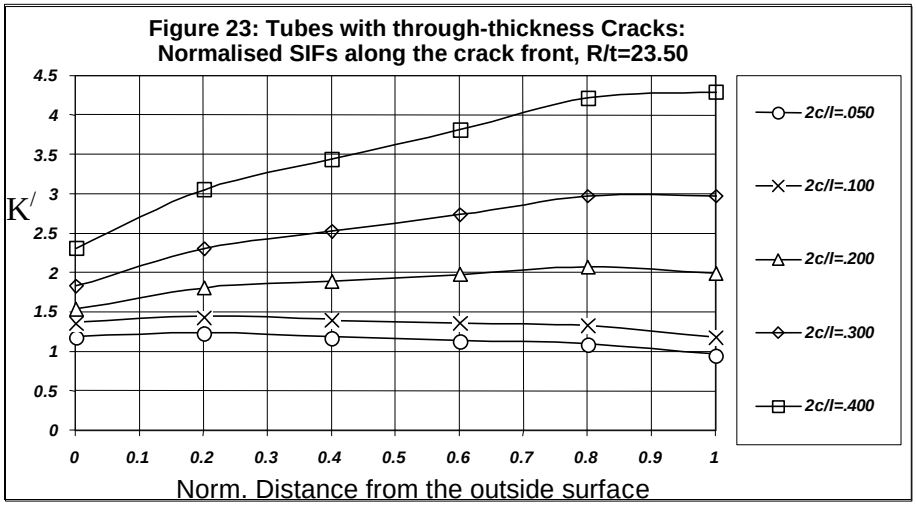
Figure 23: Tubes with through-thickness Cracks:
Normalised SIFs along the crack front, R/t=23.50
K/
4.5
4
3.5
3
2.5
2
1.5
1
0.5
0
0
0.1
0.2
0.3
0.4
0.5
0.6
0.7
0.8
0.9
1
2c/l=.050
2c/l=.100
2c/l=.200
2c/l=.300
2c/l=.400
Norm. Distance from the outside surface

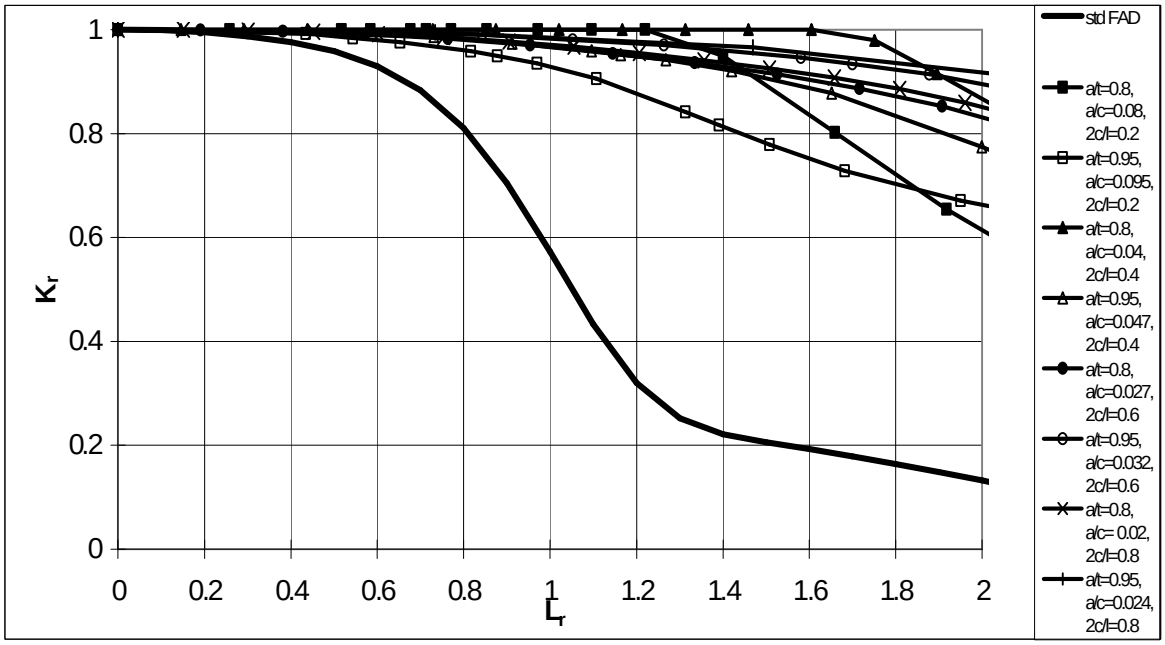

Figure 24 FADs for tubes with external semi-elliptical cracks with a/t = 0.8 and 0.95 compared to the BS 7910 Standard FAD – R/t=17

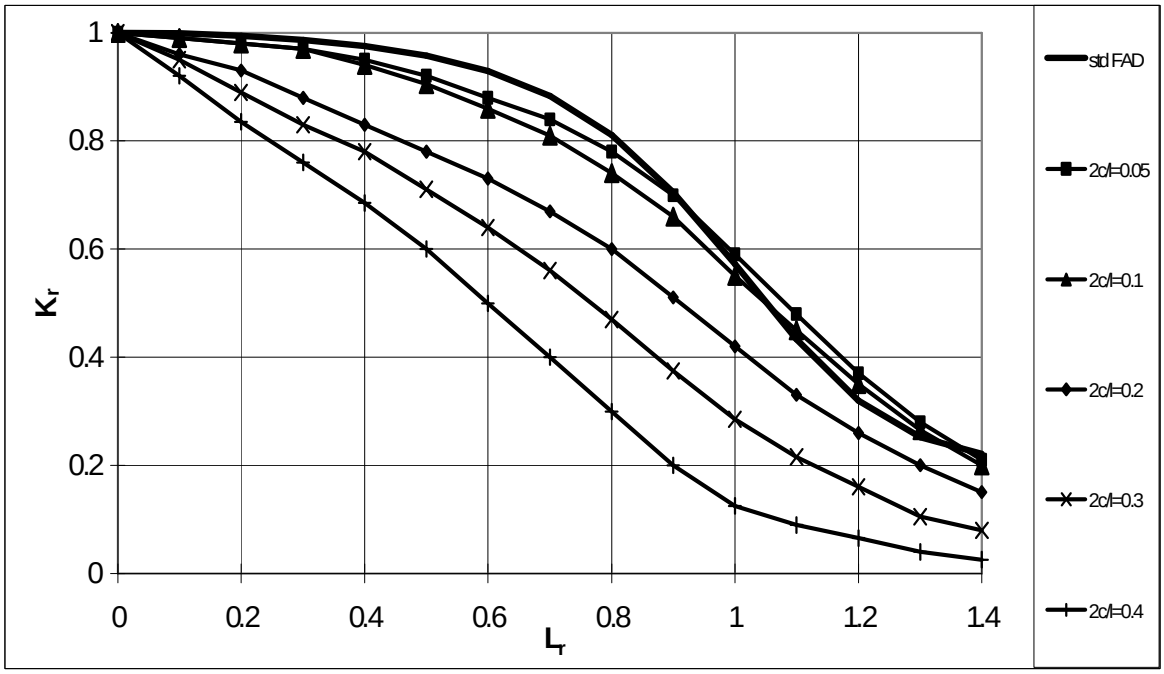

Figure 25 FADs for tubes with through thickness cracks compared to the BS 7910 Standard FAD – R/t=17

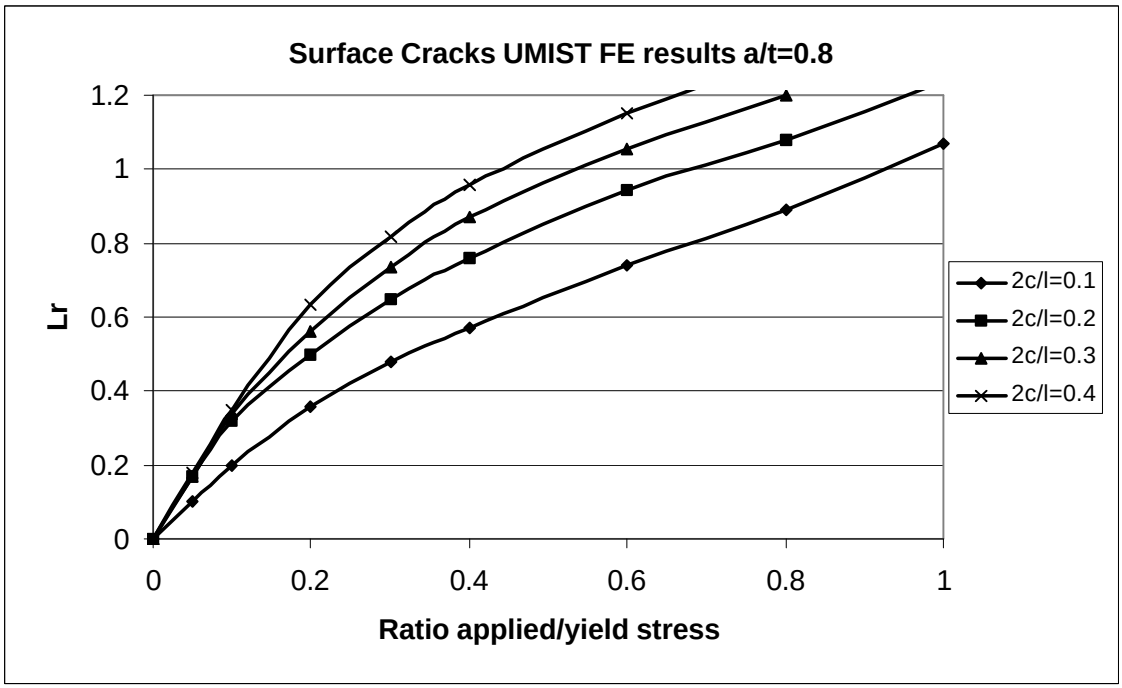

Figure 26 UMIST method for calculating L_r directly from the ratio of applied stress to yield strength for circumferential surface cracks in tubes (a/t=0.8, R/t=17)

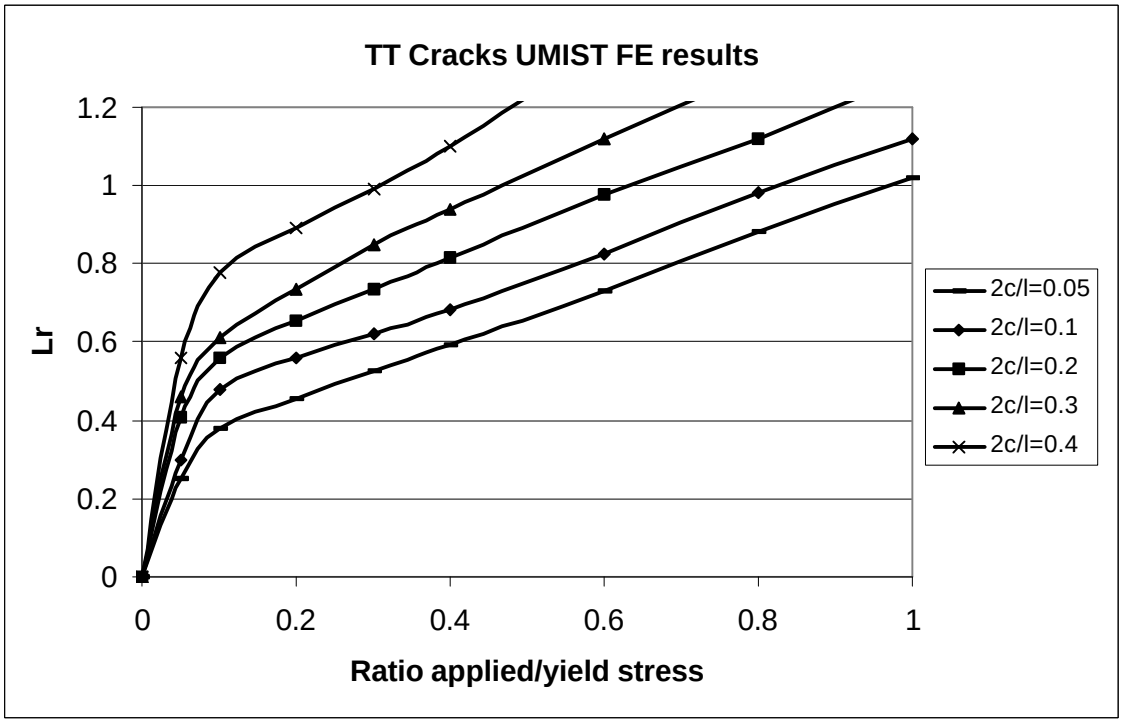

Figure 27 UMIST method for calculating L_r directly from the ratio of applied stress to yield strength for circumferential through thickness cracks in tubes (R/t=17)

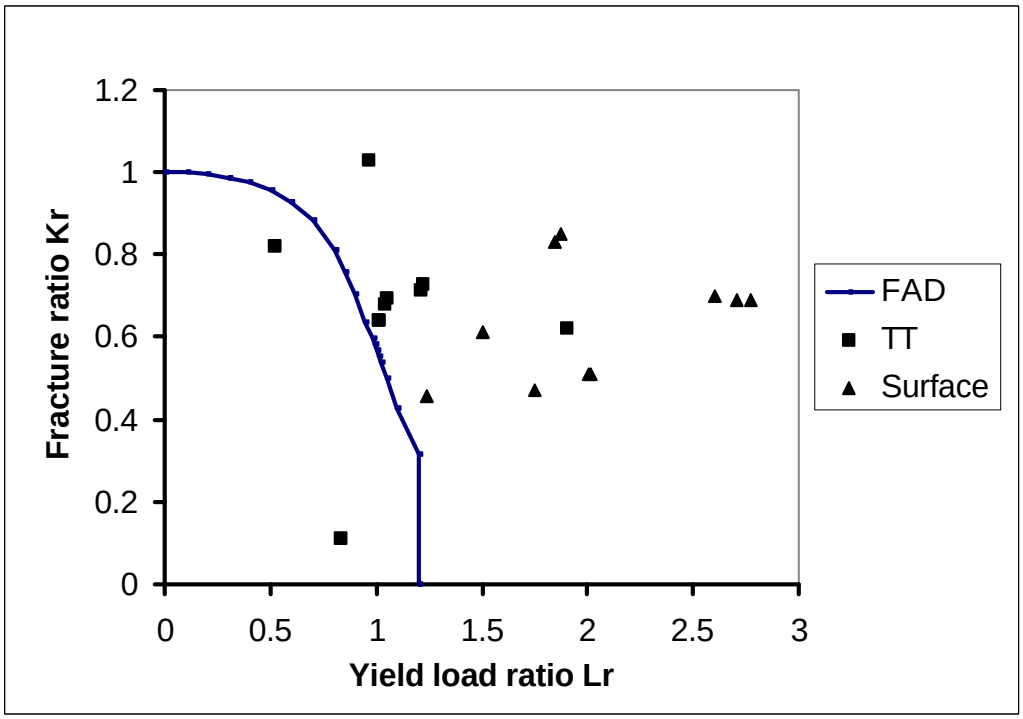

Figure 28 Results of experimental programme on circumferential cracks in tubes analysed by BS 7910 procedures using Kastner solution for L_r and based on maximum load.

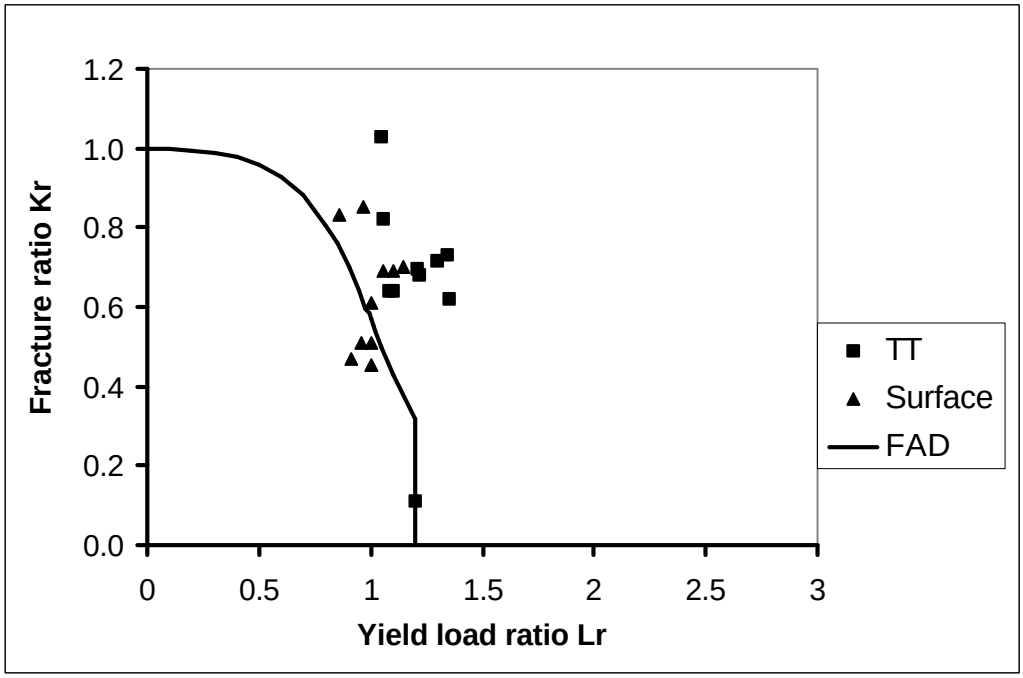

Figure 29 Results of experimental programme on circumferential cracks analysed by UMIST procedures for L_r and based on maximum load

APPENDIX A
CORRECTION FACTORS FOR CIRCUMFERENTIAL CRACKS IN TUBES

Table A1: Surface Cracks in Tubes (g = 17 cases):- Polynomial Equations relating the effective Stress Ratio ($Y=s_{eff}/s_y$) to the Nominal Applied Stress Ratio ($b=s_{app}/s_y$)

CASE	APPLIED STRESS RANGE	L_R VALUE (Y)
a/t=0.8 & 2c/l =0.1	0≤b≤1.0	$Y = -0.16340*b^6 + 0.49020*b^5 - 1.2795*b^4 + 2.8668*b^3 - 3.1593*b^2 + 2.3162*b$
a/t=0.95 & 2c/l =0.1	0≤b≤1.0	$Y = 18.546*b^6 - 54.516*b^5 + 55.725*b^4 - 18.148*b^3 - 5.5082*b^2 + 5.0717*b$
a/t=0.99 & 2c/l =0.1	B<0.05 0.05≤b≤0.1 0.1<b≤1.0	$Y = -48*b^2 + 17.2*b$ $Y = -96*b^2 + 18.4*b + 0.06$ $Y = 10.599*b^6 - 31.627*b^5 + 36.181*b^4 – 19.062*b^3 + 4.4347*b^2 – 0.05290*b +0.9167$
a/t=0.8 & 2c/l =0.2	0≤b≤1.0	$Y = -16.258*b^6 + 54.704*b^5 - 70.824*b^4 + 45.353*b^3 - 16.152*b^2 + 4.4175*b$
a/t=0.95 & 2c/l =0.2	0≤b≤1.0	$Y = -20.744*b^6 + 82.582*b^5 - 128.17*b^4 + 101.43*b^3 - 43.830*b^2 + 10.193*b +0.0078$
a/t=0.99 & 2c/l =0.2	B<0.05 0.05≤b≤0.1 0.1<b≤1.0	$Y = -216*b^2 + 30.2*b$ $Y = -48*b^2 + 9*b + 0.64$ $Y = -1.3930*b^6 + 3.9527*b^5 - 1.0946*b^4 - 2.3181*b^3 + 1.6261*b^2 – 0.12210*b +1.0588$
a/t=0.8 & 2c/l =0.3	0≤b≤1.0	$Y = 1.3072*b^6 + 3.7707*b^5 - 12.200*b^4 + 2.643*b^3 - 7.8460*b^2 + 3.9655*b$
a/t=0.95 & 2c/l =0.3	0≤b≤1.0	$Y = -53.874*b^6 + 181.78*b^5 - 242.81*b^4 +167.69*b^3 - 63.693*b^2 + 12.975*b$
a/t=0.99 & 2c/l =0.3	B<0.025 0.025≤b≤0.05 0.05<b≤1.0	$Y = -1090.3*b^2 + 59.134*b + 0.0265$ $Y = 8.4*b + 0.62$ $Y = -31.561*b^6 + 105.06*b^5 - 135.38*b^4 + 88.570*b^3 - 30.325*b^2 + 5.1988*b +0.849$
a/t=0.8 & 2c/l =0.4	0≤b≤1.0	$Y = -11.846*b^6 + 35.058*b^5 - 35.956*b^4 +18.992*b^3 - 8.4394*b^2 + 4.2741*b –0.0016$
a/t=0.95 & 2c/l =0.4	0≤b≤1.0	$Y = -36.959*b^6 + 133.49*b^5 - 193.41*b^4 +146.86*b^3 - 60.799*b^2 + 13.300*b –0.0074$
a/t=0.99 & 2c/l =0.4	B<0.0125 0.0125≤b≤0.1 0.1<b≤1.0	$Y = -3520.*b^2 + 95.6*b$ $Y = 1360.4*b^3 – 329.41*b^2 + 27.525*b + 0.3519$ $Y = 31.250*b^6 - 99.407*b^5 + 119.06*b^4 – 64.232*b^3 + 15.990*b^2 – 1.1082*b +1.1743$

Table A2: Through-thickness Cracks in Tubes: Polynomial Equations relating the effective Stress Ratio ($Y=s_{eff}/s_y$) to the Nominal Applied Stress Ratio ($b=s_{app}/s_y$)

CASE	APPLIED STRESS RANGE	L_R VALUE (Y)
γ=11 & 2c/l=0.05	0≤b≤1.00	$Y = -1.1945*b^6 + 4.9359*b^5 - 9.9341*b^4 + 11.883*b^3 - 7.8369*b^2 + 3.1713*b$
γ=11 & 2c/l=0.1	0≤b≤1.00	$Y = -15.282*b^6 + 58.325*b^5 - 87.321*b^4 + 65.221*b^3 - 25.398*b^2 + 5.5757*b + 0.005$
γ=11 & 2c/l=0.2	0≤b≤1.00	$Y = -38.374*b^6 + 132.26*b^5 - 177.28*b^4 + 117.69*b^3 - 40.725*b^2 + 7.785*b$
γ=11 & 2c/l=0.3	0≤b≤1.00	$Y = -415.57*b^6 + 975.19*b^5 - 890.53*b^4 + 401.96*b^3 - 94.502*b^2 + 12.095*b$
γ=11 & 2c/l=0.4	0≤b≤1.00	$Y = -1114.2*b^6 + 2354.1*b^5 - 1895.6*b^4 + 745.82*b^3 - 151.01*b^2 + 16.203*b$
γ=17 & 2c/l=0.05	B<0.05 0.05≤b≤1.0	$Y = 5*b$ $Y = -26.564*b^6 + 89.552*b^5 - 118.29*b^4 + 77.549*b^3 - 26.218*b^2 + 4.9404*b + 0.063$
γ=17 & 2c/l=0.1	B<0.05 0.05≤b≤1.0	$Y = 6*b$ $Y = -37.926*b^6 + 131.89*b^5 - 179.82*b^4 + 121.41*b^3 - 41.961*b^2 + 7.5143*b + 0.0205$
γ=17 & 2c/l=0.2	B<0.05 0.05≤b≤1.0	$Y = 8*b$ $Y = 14.982*b^5 - 39.443*b^4 + 39.228*b^3 - 18.176*b^2 + 4.6202*b + 0.2178$
γ=17 & 2c/l=0.3	B<0.05 0.05≤b≤1.0	$Y = 9*b$ $Y = 54.999*b^5 - 110.20*b^4 + 83.604*b^3 - 30.121*b^2 + 6.1592*b + .2088$
γ=17 & 2c/l=0.4	B<0.05 0.05≤b≤1.0	$Y = 11*b$ $Y = 438.62*b^5 – 666.27*b^4 + 389.5*b^3 – 107.86*b^2 + 14.927*b + .0287$
γ=23.5 & 2c/l=0.05	B<0.05 0.05≤b≤1.0	$Y = 5.6*b$ $Y = -2.8761*b^6 + 12.501*b^5 - 20.554*b^4 + 16.959*b^3 - 7.8455*b^2 + 2.7249*b + 0.1613$
γ=23.5 & 2c/l=0.1	B<0.05 0.05≤b≤1.0	$Y = 7.6*b$ $Y = -0.9861*b^6 + 7.4206*b^5 - 17.668*b^4 + 20.01*b^3 - 11.688*b^2 + 3.869*b + 0.2129$
γ=23.5 & 2c/l=0.2	B<0.05 0.05≤b≤1.0	$Y = 9.5*b$ $Y = -9.9418*b^6 + 52.447*b^5 - 93.953*b^4 + 78.272*b^3 - 32.427*b^2 + 6.898*b + 0.2036$
γ=23.5 & 2c/l=0.3	B<0.05 0.05≤b≤1.0	$Y = 12.6*b$ $Y = 30.563*b^6 - 22.639*b^5 - 34.054*b^4 + 47.164*b^3 - 20.667*b^2 + 4.4755*b + 0.4531$
γ=23.5 & 2c/l=0.4	B<0.05 0.05≤b≤1.0	$Y = 14*b$ $Y = -929.41*b^6 + 1739.3*b^5 - 1258.6*b^4 + 455.49*b^3 - 88.216*b^2 + 9.7023*b + 0.3858$

Printed and published by the Health and Safety Executive
C0.50 3/02

MAIL ORDER
HSE priced and free
publications are
available from:
HSE Books
PO Box 1999
Sudbury
Suffolk CO10 2WA
Tel: 01787 881165
Fax: 01787 313995
Website: www.hsebooks.co.uk

RETAIL
HSE priced publications
are available from booksellers

HEALTH AND SAFETY INFORMATION
HSE InfoLine
Tel: 08701 545500
Fax: 02920 859260
e-mail: hseinformationservices@natbrit.com
or write to:
HSE Information Services
Caerphilly Business Park
Caerphilly CF83 3GG

HSE website: www.hse.gov.uk

OTO 2001/080

£10.00

ISBN 0-7176-2301-7

9 780717 623013